

**TIME-FREQUENCY JAMMER EXCISION FOR
MULTI-CARRIER SPREAD SPECTRUM USING
ADAPTIVE FILTERING**

by

Brenno Beserra Coelho

B.S. E.E., Federal University of Maranhao, Brazil, 2000

Submitted to the Graduate Faculty of
the School of Engineering in partial fulfillment
of the requirements for the degree of

Master of Science

University of Pittsburgh

2006

UNIVERSITY OF PITTSBURGH
SCHOOL OF ENGINEERING

This thesis was presented

by

Brenno Beserra Coelho

It was defended on

July 21st 2006

and approved by

Luis F. Chaparro, Associate Professor of Electrical and Computer Engineering

Amro A. El-Jaroudi, Associate Professor of Electrical and Computer Engineering

Heung-no Lee, Assistant Professor of Electrical and Computer Engineering

Thesis Advisor: Luis F. Chaparro, Associate Professor of Electrical and Computer
Engineering

Copyright © by Brenno Beserra Coelho
2006

TIME-FREQUENCY JAMMER EXCISION FOR MULTI-CARRIER SPREAD SPECTRUM USING ADAPTIVE FILTERING

Brenno Beserra Coelho, M.S.

University of Pittsburgh, 2006

The development of new wireless technologies, the improvement of existing ones and the reduction on the wireless devices prices are increasing the number of users, the demand for bandwidth and the demand for higher data rates. The spread of the technology however brings some drawbacks. One is the increasing interference level that can degrad the wireless communications. Many different techniques are used to minimize the interference and the effect of the channel (multipath, Doppler etc) in a wireless channel. This thesis considers the frequency and time processing of a jammer affected *multi-carrier spread spectrum* (MC-SS) system. A linear chirp is used as a spreading sequence. Such a sequence not only provides a constant envelope, but also allows the estimation of the channel parameters using a linear time-invariant model. Hence time-delays and Doppler frequency shifts can be represented by effective time shifts. The *discrete evolutionary transform* (DET) time-frequency representation is used for estimating the channel characteristics and for detecting jammers. Once the jammers are detected, the original spreading function corresponding to the jammed frequency is adapted to minimize the jammer effects. The bit detection is then performed using a least mean square (LMS) adaptive filter and it is done in both time- and frequency-domains. To illustrate the performance of the method, simulations with different signal to noise ratios, different jammer to signal ratios and different Doppler shifts were performed. The results indicate that the method is capable of excising the jammers providing a good bit error rate in low Doppler situations.

Keywords: Multipath channel fading, Multicarrier spread spectrum, Discrete evolutionary transform, complex quadratic sequence, Doppler shifts, Channel modeling, adaptive filter, Jammer excision.

TABLE OF CONTENTS

PREFACE	xi
1.0 INTRODUCTION	1
1.1 Motivation and Scope	1
1.2 Dissertation Overview	2
2.0 MULTICARRIER SPREAD SPECTRUM	4
2.1 Orthogonal Frequency Division Multiplexing - OFDM	4
2.2 Spread Spectrum	9
2.2.1 Direct Sequence Spread Spectrum - DSSS	10
2.2.2 Frequency Hopping Spread Spectrum - FHSS	12
2.3 Multi-Carrier Spread Spectrum	13
2.4 Channel Modeling	15
2.4.1 Multipath Fading	16
2.5 Channel Characterization and Modeling	20
2.6 LMS Filter	22
2.6.1 LMS Algorithm	23
2.7 Jamming Signals	24
2.7.1 Jammer Waveforms	25
2.7.1.1 Broadband and Partial-Band Noise Jammers	25
2.7.1.2 Continuous Wave and Multitone Jammers	26
2.7.1.3 Pulse Jammer	27
2.7.1.4 Chirp Jammer	28
3.0 CHANNEL ADAPTIVE ESTIMATION IN MC-SS	29

3.1	Channel Model	30
3.2	Jammer Detection	32
3.3	Channel Estimation	34
3.3.1	Multipath Estimation using Discrete Evolutionary Transform (DET)	35
3.4	Adaptation for Channel Estimation	38
3.5	Bit Detection	39
3.5.1	Frequency-Domain Bit Detection without Channel Estimation	40
3.5.2	Frequency-Domain Bit Detection with Channel Estimation	41
3.5.3	Time-Domain Bit Detection without Channel Estimation	42
3.5.4	Time-Domain Bit Detection with Channel Estimation	44
3.6	Simulations	45
4.0	CONCLUSIONS	55
4.1	Future Work	56
	APPENDIX. MATLAB CODE	57
	BIBLIOGRAPHY	64

LIST OF TABLES

1	The LMS Algorithm for p^{th} -order FIR adaptive filter	24
---	---	----

LIST OF FIGURES

1	OFDM waveform using rectangular pulse	6
2	OFDM spectrum	7
3	Ideal OFDM model	9
4	Model of spread-spectrum digital communications system	10
5	DSSS coding	12
6	FHSS coding	13
7	DSSS and FHSS comparison	14
8	Channel effect on Multi-carrier	15
9	Channel fading (taken from [2])	18
10	Mobile unit moving at speed v	20
11	Time variation of the channel	21
12	Block diagram of an adaptive filter	22
13	Broadband jammer in frequency domain	26
14	Partial jammer in frequency domain	26
15	CW jammer in frequency domain	27
16	Multitone Jammer in frequency domain	27
17	Chirp jammer in time-domain	28
18	Multicarrier spread spectrum	30
19	MC-SS frequency sub-channel	32
20	Time-Frequency Analysis	33
21	Model of LMS adaptive filter	40
22	Comparison between approaches in the frequency-domain	46

23	BER vs SNR frequency-domain without Doppler	47
24	BER vs SNR frequency-domain with Doppler = 0.001π	48
25	BER vs SNR frequency-domain with Doppler = 0.01π	48
26	Comparison time-domain with and without jammer detection, JSR=0dB . . .	49
27	Comparison time-domain with and without channel estimation	49
28	BER vs SNR time-domain without Doppler	50
29	BER vs SNR time-domain with Doppler = 0.001π	51
30	BER vs SNR time-domain with Doppler = 0.01π	51
31	BER vs SNR time- vs frequency-domain without Doppler JSR=-2 dB	52
32	BER vs SNR time- vs frequency-domain with Doppler= 0.01π JSR=-2 dB . .	52
33	Algorithm frequency-domain detector flow chart	53
34	Algorithm time-domain detector flow chart	54

PREFACE

I would like to thank my advisor Professor. Luis F. Chaparro for the guidance and support he has provided me throughout my M.S. studies. I would like also to express my appreciation to Professor Jaroudi and Professor Lee, members of my dissertation committee for their time and invaluable feedback.

I am also grateful to my friends and colleagues The Ferreiras, Rodrigo Duailibe, Seda Senay, Luciano Lima and Guilherme Aragao.

I would like to express my gratitude to the Alcoa Foundation for sponsoring my graduate studies and to the Center for Latin American Studies - University of Pittsburgh.

Finally, my regards to Yuka Morishita for her companionship during my stay in US, my sister Lenina and my brother Daniel for their support. I dedicate this dissertation to my parents for all they have done for me.

1.0 INTRODUCTION

1.1 MOTIVATION AND SCOPE

The development of mobile phones, wireless computer networks, etc, is making wireless communications become a part of almost everyone's life. The technology is spreading throughout the world in many different applications. In the past, most of the wireless communications used light as a way of transmission. The light was either "modulated" using mirrors or flags were used to signal code words [3]. However, optical transmission needs line-of-sight paths and suffers from the high frequency of the carrier, and rain and fog degrade the communication capacity.

Wireless communications technology truly began with the discovery of electromagnetic waves and the development of equipments to modulate them. It started when Michael Faraday in 1831 demonstrated the electromagnetic induction and James C. Maxwell from 1831 to 1879 laid the theoretical foundations for electromagnetic fields. Then Heinrich Hertz in 1857-1894 proved the Maxwell equations demonstrating the wave character of electrical transmission through space.

One of the major limitations in mobile wireless communications is the fading due to multi-path [2]. Multi-path causes the signal to have multiple delayed versions of itself with different attenuations, time delays and phase shift. The channel characteristics are also time-variant due to the mobility of the user or changes in the environment. The mobility of users can cause the Doppler effect degrading the channel even more. Those characteristics make the wireless channel a harsh environment for communications.

In this thesis we consider the multicarrier spread spectrum technique using a linear chirp sequence as the spreading function. The channel characteristics, such as number of paths,

attenuation and Doppler, are random and change after each sent message. An adaptive filter is used to perform the bit detection. To improve the results, channel estimation is performed using the discrete evolutionary transform and its results are used as an input to the adaptive filter. We show the detection results using a time- and a frequency-domain technique.

1.2 DISSERTATION OVERVIEW

The research presented in this work is primarily concerned with the effects of jammers and noise on a wireless transmission. The channel is modeled as a multipath channel characterized by delays, attenuations and Doppler shifts. Two different approaches are taken to detect the sent bit, one is based on the frequency-domain while the other one is based on the time-domain representation of the received signal. Both methods use a time-frequency representation of the signal to detect the frequencies where jammers are present. This step is taken prior to the bit detection and uses the *discrete evolutionary transform* (DET) as the time-frequency representation. DET is one of the different time-frequency analysis method.

This thesis is organized as follows. In Chapter 2 the necessary theoretical background is introduced, such as orthogonal frequency division multiplexing, spread spectrum communications, linear time-varying (LTV) and linear time-invariant (LTI) channel models, multipath channel fading and least mean square (LMS) adaptive filters. The chapter also describes the DET method and explains how channel estimation is performed. Finally, it describes the different types of jammers.

Chapter 3 introduces the linear chirp spreading sequences $g(n)$ and describes their characteristics. After that, channel modeling is presented. After introducing channel modeling, we present the jammer detection process which uses the DET to determine frequencies where a jammer is present. Section 3.3 describes the channel estimation method where the channel characteristics are estimated while the following section presents the adaptation method that is used to minimize the jammer effects on the channel estimation. Section 3.5 explains the methods used to estimate the sent bit. Several simulations are presented using both time and frequency-domain. Also a comparison is made between bit estimation using channel

information (obtained through channel estimation) and without using channel estimation. Finally, a general conclusion with the contributions of this thesis and some ideas for future work are provided. In this work, a single user case is considered. It is also assumed that there is perfect synchronization between sender and receiver.

2.0 MULTICARRIER SPREAD SPECTRUM

Multi-carrier modulation (MCM) is a technique of transmitting data using multiple parallel low-rate sub-streams instead of a serial high-rate stream. Each sub-stream is then modulated using a different carrier frequency [4]. The advantages of MCM include relative immunity to fading caused by transmission over more than one path at a time (multipath fading), less susceptibility than single-carrier systems to interference caused by impulse noise [5], and enhanced immunity to inter-symbol interference. Limitations include difficulty in synchronizing the carriers under marginal conditions, and a relatively strict requirement that amplification needs to be linear. In this Chapter, we present an overview of multi-carrier methods.

2.1 ORTHOGONAL FREQUENCY DIVISION MULTIPLEXING - OFDM

The first introduced multicarrier technique was the *Orthogonal Frequency Division Multiplexing* (OFDM), proposed in the 60's by Chang [6]. He presented a principle for transmitting messages simultaneously through a linear bandlimited channel without *interchannel* (ICI) and *intersymbol interference* (ISI). In 1971, Weinstein and Ebert [7] introduced the *discrete Fourier transform* (DFT) as a way to perform the multicarrier modulation and demodulation. To combat ISI and ICI they used both a guard space between the symbols and a raised-cosine windowing in the time domain. Despite the fact that their system did not obtain perfect orthogonality between subcarriers, it was an important contribution to OFDM. In 1980, Peled and Ruiz [8] introduced the *cyclic prefix* (CP). The cyclic prefix is actually a copy of the last portion of the data symbol appended to the front of the symbol during the guard interval. It

is sized appropriately to serve as a guard time to eliminate ISI. This is accomplished because the amount of time dispersion from the channel is smaller than the duration of the cyclic prefix.

One of the major OFDM assets is its simplicity. OFDM consists basically of a serial-parallel converter, so that a high-rate stream is converted into N low-rate sub-streams, which are then modulated with different carriers. The carrier spacing has to be carefully chosen to guarantee orthogonality, allowing the receiver to separate the different carriers. The N sub-carriers are then added, modulated up to the transmit frequency and sent out across the channel [9].

To understand the benefits of OFDM it is necessary to consider the transmission over the channel. The original signal has a high data rate, therefore has a small symbol period. Since frequency and period are inversely proportional, a small period results in a large bandwidth. The large bandwidth can lead to frequency selectivity. This means that the sent signal will not have a constant gain within the message bandwidth. To mitigate the frequency selectivity a more complex receiver would be required. Using OFDM, N low rate streams are sent, each with a narrow bandwidth experiencing a flat fade. In a flat fade channel, the gain is constant over a certain bandwidth. As a result, a simpler receiver can be used.

The subcarrier pulse used for transmission is usually chosen to be rectangular in the time-domain. Using a rectangular pulse has an advantage that the task of pulse forming and modulation can be performed by a simple Inverse Discrete Fourier Transform (IDFT). Recently, the interest in using different pulses has increased. By using different kind of pulses, one can get a spectrum that can be more suitable for different applications, which can be beneficial from interference point of view. Figure 1 shows the frequency representation of an OFDM waveform using rectangular pulse.

A multicarrier systems transmits N complex-valued source symbols S_n on N subcarriers. Source symbols are obtained after source and channel coding, interleaving, and symbol mapping. The source symbol duration T_d of the serial data symbols results after serial-to-parallel conversion in the OFDM symbol duration $T_s = NT_d$ in binary modulation. Serial-to-parallel conversion is then followed by an N sub-stream modulation onto subcarriers with a spacing

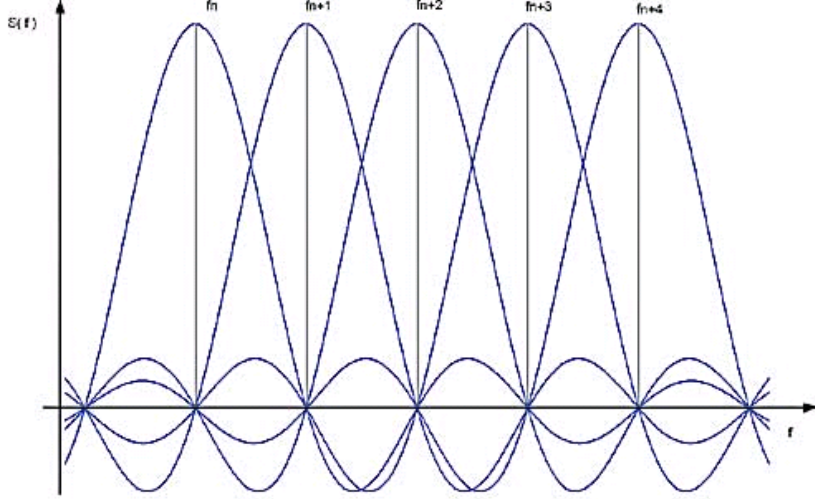


Figure 1: OFDM waveform using rectangular pulse

of F_s to achieve orthogonality. F_s is given by

$$F_s = \frac{1}{T_s},$$

the complex envelope of an OFDM symbol with rectangular pulse shaping has the form

$$x(t) = \frac{1}{N} \sum_{n=0}^{N-1} S_n e^{j2\pi f_n t},$$

the N subcarriers frequencies are located at $f_n = \frac{n}{T_s}$, for $n = 0, 1, \dots, N-1$. The symbols are all transmitted with the same power. When one uses large values of N , the *power density spectrum* (pds) becomes flatter in the normalized frequency range of $-0.5 \ll fT_d \ll 0.5$ (see Figure 2) containing the N subchannels [4]. It is important to emphasize that only subchannels near the band edges contribute to the out-of-band power emission. As said before, OFDM allows using IDFT to implement the multicarrier modulation. If the complex envelope $x(t)$ is sampled with rate $\frac{1}{T_d}$ one gets

$$x_\nu = \frac{1}{N} \sum_{n=0}^{N-1} S_n e^{j\frac{2\pi n\nu}{N}} \quad \nu = 0, 1, \dots, N-1,$$

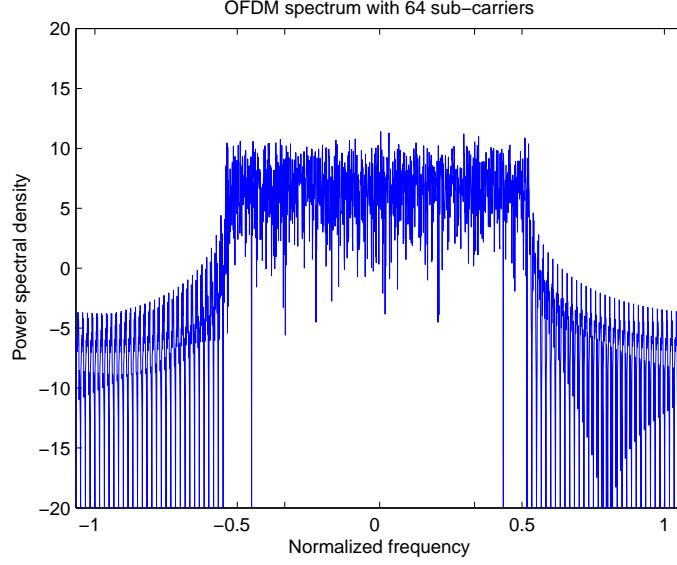


Figure 2: OFDM spectrum

If N is large, its pds will approach a single carrier modulation spectrum. Furthermore, the OFDM symbol duration T_s becomes large compared to the channel impulse response period, reducing the amount of ISI. The duration of an OFDM's guard interval is $T_g \gg \tau_{max}$, where τ_{max} is the maximum in the channel delay. The use of a guard interval or cyclic prefix inserted between symbols allows to completely avoid ISI maintaining the orthogonality, hence avoiding ICI, between the subcarriers signals [4]. The CP is obtained by extending the duration of an OFDM symbol to $T'_s = T_g + T_s$. The length of the guard interval in samples is given by the ceiling function

$$L_g \geq \left\lceil \frac{\tau_{max}N}{T_s} \right\rceil,$$

and the sampled sequence with cyclic guard interval will be

$$x_\nu = \frac{1}{N} \sum_{n=0}^{N-1} S_n e^{j\frac{2\pi n\nu}{N}} \quad \nu = -L_g, \dots, N-1,$$

x_ν is then converted into an analog signal and sent out over the channel.

The channel affects the sent signal (multipath, Doppler, etc) resulting in a received signal $y(t)$, that is the superposition of the sent signal and the channel impulse response plus the addition of noise.

$$y(t) = \int_{-\infty}^{\infty} x(t - \tau)h(\tau, t)d\tau + \eta(t)$$

where $h(\tau, t)$ and $\eta(t)$ are the channel's impulse response and white noise. The signal $y(t)$ is then passed through a analog-to-digital converter getting as output a signal y_ν , where $\nu = -L_g, \dots, N - 1$. That means that y_ν is a sampled version of the signal $y(t)$ sampled at a rate $1/T_d$. The first L_g samples are removed since ISI is present, and a DFT is performed on the rest of the signal to get the multi-carrier demodulated sequence R_n , $n = 0, \dots, N - 1$.

$$R_n = \sum_{\nu=0}^{N-1} y_\nu e^{-j\frac{2\pi n\nu}{N}}, \quad n = 0, \dots, N - 1,$$

One can consider each sub-channel separately, since guard interval avoids ICI. Therefore, for each sub-carrier the received symbol frequency representation is given by [4]

$$R_n = H_n S_n + N_n, \quad n = 0, \dots, N - 1,$$

where H_n and N_n represent the channel and the noise of the n th sub-channel. Figure 3 shows an OFDM system

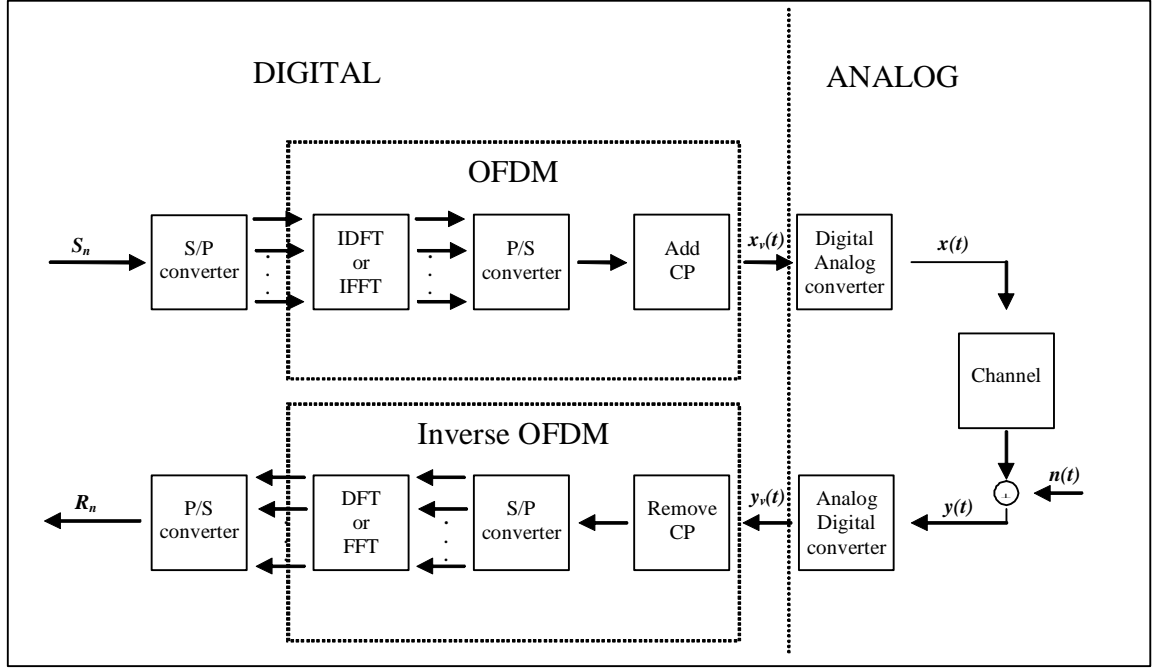


Figure 3: Ideal OFDM model

2.2 SPREAD SPECTRUM

Multicarrier spread spectrum (MCSS) can be described as a combination of OFDM and spread spectrum techniques [10]. Therefore a brief overview of spread spectrum is necessary. *Spread spectrum* (SS) has been under development for more than 50 years (started in mid 50's). The system spreads the signal energy over a bandwidth much greater than the signal information bandwidth [11]. As a result of the spreading process, the spectral power spectral density (Watts per Hertz) is very small. This low transmitted power density characteristic gives spread signals a great advantage since spread and narrow band signals can occupy the same band, with little or no interference. Spread Spectrum is useful for [11]

- Signal hiding and noninterference with conventional systems
- Anti-jam and interference rejection
- Privacy

- Multiple access
- Multipath mitigation

Spreading results directly in the use of a wider frequency band, so it does not spare the limited frequency resource. That overuse is well compensated, however, by the possibility that many users will share the enlarged frequency band. The main parameter in a spread spectrum system is the processing gain, $P_g = B/B_s$, which is the ratio between the transmission bandwidth B and the information bandwidth B_s . The higher P_g , the lower the power density one needs to transmit the information. For a large bandwidth, the transmitted signal spectrum looks like noise.

The main components of a spread spectrum digital communication system are illustrated in Figure 4. It consists of basic elements of a conventional digital communication system plus two synchronized pseudorandom sequence generators. These two generators produce a *pseudorandom* or *pseudonoise* (PN) binary-valued sequence which is used to spread the transmitted signal at the modulator and to despread the received signal at the demodulator. Time synchronization of the PN sequence generated at the transmitter with the PN sequence at in the receiver signal is required in order to properly despread the received spread-spectrum signal.

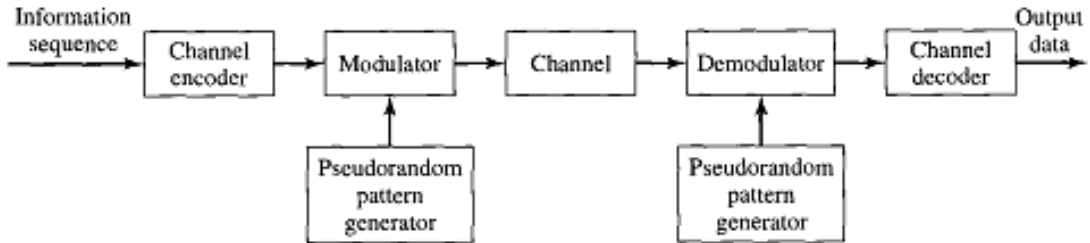


Figure 4: Model of spread-spectrum digital communications system

2.2.1 Direct Sequence Spread Spectrum - DSSS

There are two major ways to spread the spectrum: *direct sequence* (DSSS) and *frequency hopping* (FHSS). In the DSSS technique, the PN sequences are applied directly to data

entering the carrier modulator. The modulator therefore sees a much larger bit rate, which corresponds to the chip rate of the PN sequence (Figure 5). The result of modulating an RF carrier with such a code sequence is to produce a direct-sequence-modulated spread spectrum with $(\sin(x)/x)^2$ frequency spectrum, centered at the carrier frequency. The information-bearing baseband signal $m(t)$, which is transmitted at a rate R , and has the duration period of $T_b = 1/R$ seconds can be expressed as [2]

$$m^{(k)}(t) = \sum_{i=-\infty}^{\infty} d_i^{(k)} g(t - iT_b),$$

where $d_i^{(k)} = \pm 1$ and $g(t)$ is a rectangular pulse of duration T_b . Using a spreading sequence $p^{(k)}(t)$ of length L ,

$$p^{(k)}(t) = \sum_{l=0}^{L-1} c_l^{(k)} g_{T_c}(t - lT_c),$$

to each user k , $k = 0, \dots, K-1$, for K is the number of users and $g_{T_c}(t)$ (rectangular pulse) equal to 1 for a interval $[0, T_c)$ and zero otherwise. T_c is the chip duration and $c_l^{(k)}$ are the chips that belong to a user's spreading sequence. The output for each data symbol with duration $T_d = LT_c$ will be given by

$$\begin{aligned} x^{(k)}(t) &= d^{(k)} \sum_{l=0}^{L-1} c_l^{(k)} g_{T_c}(t - lT_c), \quad 0 \leq t < T_d, \\ &= m^{(k)}(t) p^{(k)}(t), \end{aligned}$$

and

$$\begin{aligned} x(t) &= \sum_{k=0}^{K-1} x^{(k)}(t), \\ &= m(t) p(t), \end{aligned}$$

Finally, the signal $x(t)$ is used to modulate the carrier $A_c \cos(2\pi f_c t + \theta)$. The transmitted signal can be written as

$$s(t) = A_c m(t) p(t) \cos(2\pi f_c t + \theta),$$

however, for any t , $x(t) = \pm 1$, thus, the modulated transmitted signal can be expressed as

$$s(t) = A_c \cos(2\pi f_c t + \theta(t)),$$

where $\theta(t) = 0$ or π . Hence, the carrier modulated transmitted signal is a *binary phase shift keying* (BPSK) signal. The received signal, $r(t)$, is multiplied by the PN code and then filtered. This process results in a correlator. The signal is then passed through a BPSK demodulator to recover the original data. DSSS is also known as *direct sequence code division multiple access* (DS-CDMA) and it is the best known spread spectrum technique.

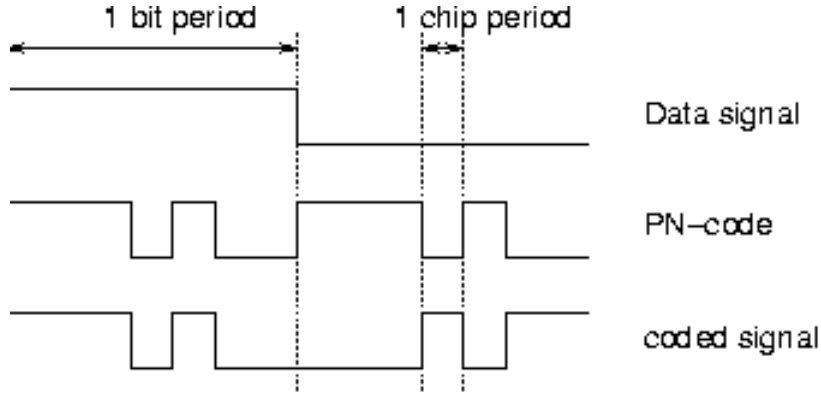


Figure 5: DSSS coding

2.2.2 Frequency Hopping Spread Spectrum - FHSS

Another spreading method widely used is the FHSS, this method causes the carrier to hop from frequency to frequency over a wide band according to a sequence defined by the PN of length L_{fh} , see Figure 6. In this way the bandwidth is increased by a factor L_{fh} (non-overlapping channels). The speed at which hops are executed depends on the data rate of the original information. A disadvantage of frequency-hopping, as opposed to direct-sequence, is that obtaining a high processing-gain is difficult. There is the need for a frequency-synthesizer able to perform fast-hopping over the carrier-frequencies. The faster the hopping-rate is, the higher the processing gain.

The transmitted spectrum of a frequency hopping signal is quite different from that of a direct sequence system. Instead of a $(\sin(x)/x)^2$ shaped envelope, the frequency hopper's output is flat over the band of frequencies used. Figure 7 shows the difference between DSSS

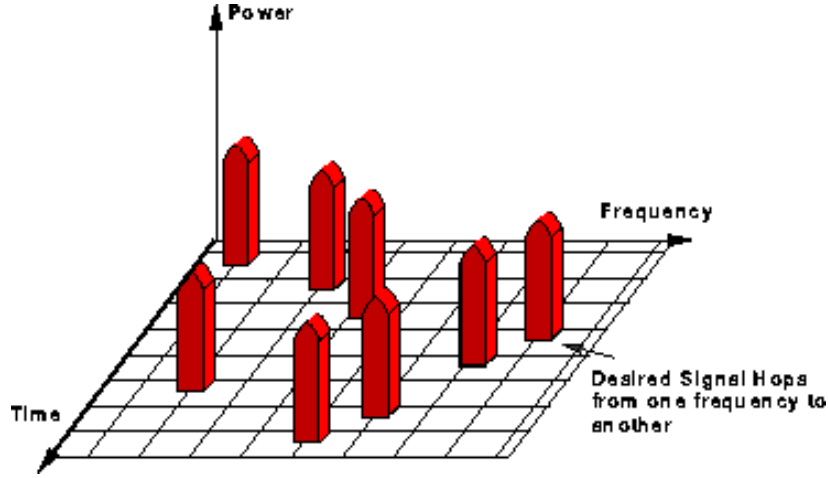


Figure 6: FHSS coding

and FHSS modulation. The former applies the PN sequence to the data (DATA in the figure) while the later uses the PN sequence to determine the frequency hops (LO in the figure).

2.3 MULTI-CARRIER SPREAD SPECTRUM

The basic principle of the combination between OFDM and spread spectrum that results in the MC-SS is straightforward: it spreads the transmitting signal in frequency so that one copy of the transmitting signal is sent in each sub-carrier. In other words, a user sends his data over N sub-carriers simultaneously with another user over the same N sub-carriers. To avoid collision between data sent by each user, a coding technique is applied and so the data is separable at the receiver. This is done by applying a unique code to each user for all N sub-carriers.

MC-SS can outperform direct-sequence spread spectrum system for some jammers [12] and by means of a cyclic guard interval it is able to remove ISI just like OFDM. However, the

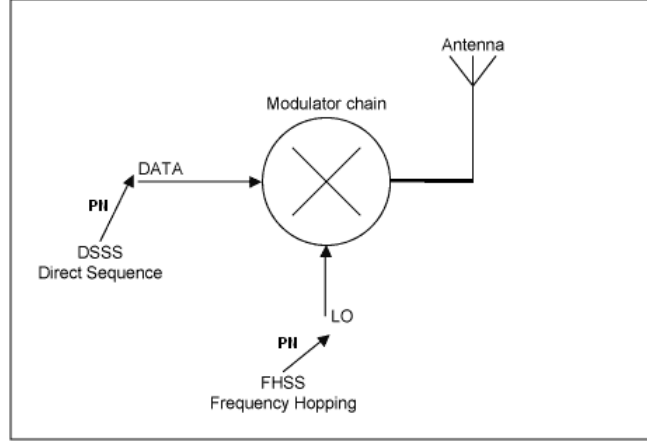


Figure 7: DSSS and FHSS comparison

complex envelop of a multi-carrier spread spectrum signal is not constant, even with BPSK or QPSK signaling. This property is due to the IDFT transform and will cause distortion when the signal is passed through a nonlinear power amplifier [13].

MC-SS is affected by the channel as follows: each of the N sub-channels has a narrow bandwidth, therefore it can be considered that a constant gain affects all the frequencies in one carrier. This phenomenon is called flat fade channel. However, what is true for one subcarrier is not true for the entire set of N sub-channels. This means that each subcarrier will be affected in a different way by the channel and so the channel is frequency selective (Figure 8).

At the receiver side, the first step is to return the received signal to the baseband. Then the signal is divided into its subcarriers components. This can be achieved by multiplying the received signal by the complex conjugate of each subcarrier followed by a low pass filter (acting as a integrator). Finally, the signal has to be "despread", each user has a different spreading code, and then combined. The combiner performs a weighted addition of the carrier terms such that:

- Minimizes the presence of other user's signal.
- Maximizes the frequency diversity benefit.
- Minimizes the presence of the noise.

Possible combiner techniques are: *equal gain combiner* (EGC), *orthogonality restoring combiner* (ORC) and *minimum mean squared error combiner* (MMSEC) [9].

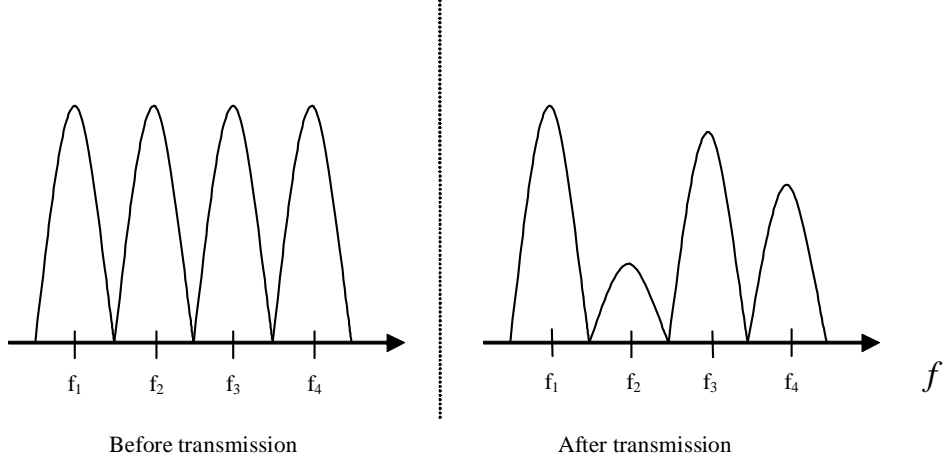


Figure 8: Channel effect on Multi-carrier

2.4 CHANNEL MODELING

In wireless communications systems a primary issue is the effects of the radio channel such as attenuation, multipath and Doppler. Those effects can increase the ISI, reduce the signal strength (attenuation) and increase the *bit error rate* (BER). A radio link is called *free space path* if the link that connects the transmitter and the receiver is free of all objects that can absorb or reflect radio frequency. In this sort of link, the received signal is attenuated by a free space path loss factor L_{free} , that is given by [14]

$$L_{free} = -20 \log_{10} \frac{\lambda}{4\pi d} \text{ dB}, \quad (2.1)$$

It can be seen that the attenuation depends basically on the distance d between the transmitter and the receiver and on the signal's wavelength λ . Therefore, the received signal can be predicted and the attenuation factor is the only channel parameter that can determine the power level of the received signal [2]. Unfortunately, the channel characteristics are not described only by its attenuation. Reflection, scattering, diffraction of the transmitted signal occur and can produce attenuation and delay in the signal. Thus the received signal strength will fluctuate around a mean or a median value. This phenomenon can be described as fading and be characterized in terms of the primary cause (multipath), the statistical distribution of the received envelope (Rayleigh, Rician or lognormal), the duration of fading (long-term or short-term) or fast versus slow fading [14].

2.4.1 Multipath Fading

A signal while propagating from the transmitter to the receiver will typically do it over multiple reflective paths. This results in fluctuations of the received signal amplitude caused by the addition of signals arriving with different phases. The phase difference is caused by the different paths (with diverse distances) that signals have traveled. It is important to characterize the kind of fading in order to analyse the channel behaviour. Two important variations are the large-scale and the small-scale fading.

1. Large-scale fading. Large scale fading is explained by the gradual loss of received signal power (since it propagates in all directions) with respect to the transmitter-receiver separation distance. However, different received signal strength can be obtained for the same distance between transmitter and receiver. This happens due to the environment and surroundings, and the location of the objects. Equation 2.1 provides the mean value of the received signal, but the actual received signal will fluctuate around this value. This fluctuation is called *shadow fading* or *slow fading*. It is called slow fading because the fluctuations around the mean due to the distance varies slower than fluctuations due to multipath [15]. The path loss equation given before can include the shadow fading

$$L_{free} = -20 \log_{10} \frac{\lambda}{4\pi d} + X,$$

where X defines the shadow fading and is given in dB. Shadow fading may not allow some locations within a given distance to receive a sufficient signal strength. Hence, an additional signal power might be necessary to overcome the shadow fading effect.

2. Small-scale fading. Small-scale fading describes the effects of small changes between a transmitter and a receiver. Three main factors impact on small-scale fading: multipath propagation (reflection, scattering and diffraction), movement of transmitter and receiver (Doppler effect), and changes and motions of objects in the environment.

As a way to model the multipath signal fluctuations, one can generate a histogram of the received signal strength in the time domain. The Rayleigh distribution is the most used to describe the multipath fading and its probability density function is given by [15]

$$f_{ray}(r) = \frac{r}{\sigma^2} e^{-\frac{r^2}{2\sigma^2}} \quad , \quad r \geq 0,$$

where r is the random variable corresponding to the signal amplitude. The Rayleigh fading corresponds to the small-scale fading since the fluctuation of the signal envelope is Rayleigh distributed when no predominant line-of-sight signal is present [2]. If a strong *line-of-sight* (LOS) component is presented, the signal distribution will be considered as a Ricean with probability density function

$$f_{ric}(r) = \frac{r}{\sigma^2} e^{\left(-\frac{r^2+K^2}{2\sigma^2}\right)} I_0 \frac{Kr}{\sigma^2} \quad , \quad r \geq 0, K \geq 0,$$

where K is a factor that determines how strong is the LOS component compared to the other multipath signals. A small value of K means that the received signal is predominantly non-LOS signal, while a large value means that the signal is basically a LOS. I_0 is the Bessel function of the first kind. Small-scale fading manifests in two ways: time dispersion and time variation of the channel. Figure 9 resumes the types of fading.

At high data rates, the symbol duration becomes really small, and the symbol becomes, in the frequency domain, wideband. Thus the channel frequency response will no longer be flat within a symbol period. This phenomenon is called time dispersion of the channel or frequency selective fading. It is possible to analyse this phenomenon either in the time or in the frequency domain.

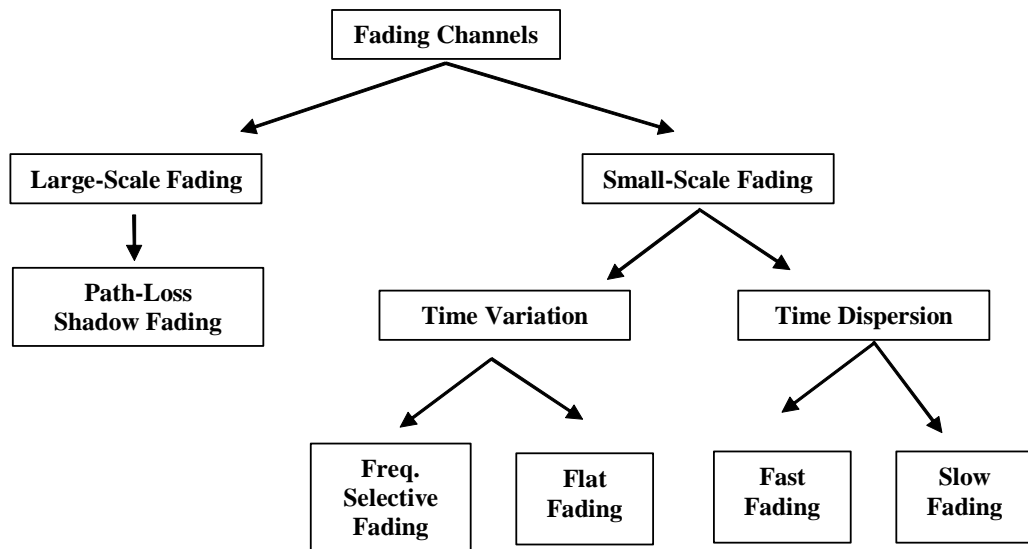


Figure 9: Channel fading (taken from [2])

The time domain view says that there are multipath components that can cause inter-symbol interference if the symbol duration is smaller than the maximum multipath delay spread.

The frequency domain approach says that there are multipath components that can cause notches in the frequency response. An important concept is the *coherence bandwidth* meaning the frequencies where the channel characteristics are constant. Time dispersion results in irreducible error rates, meaning that even if the power is infinitely increased, there will be no improvement on the bit error rate. There are some ways to overcome time dispersion such as:

- Spread Spectrum
- OFDM
- Equalization

Time variation of the channel, as the name says, means how fast the channel fades. That variation depends on how fast the mobile is moving compared to the transmitter. The motion of the mobile unit will result in a Doppler shift in the frequency of the received signal [15]. The maximum Doppler shift, f_d , is given by

$$f_d = f_0 \frac{\nu}{c},$$

where c is the electromagnetic wave speed in free space, ν is the speed of the mobile receiver and f_0 is the carrier frequency. If one takes all possible directions, the instantaneous frequency f_{in} can be written as

$$f_{in} = f_0 + f_d \cos(\theta_i), \tag{2.2}$$

where θ_i is the angle of arrival (see Figure 10). An example of a Doppler-faded signal can be seen in Figure 11. As the coherence bandwidth in the time dispersion, coherence time of a channel is the average time for which the channel can be assumed to be constant.

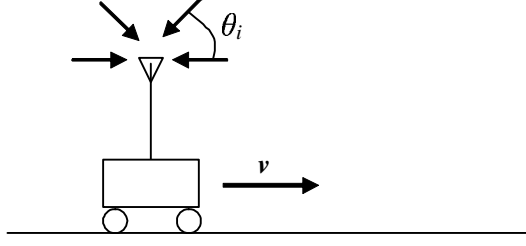


Figure 10: Mobile unit moving at speed v

2.5 CHANNEL CHARACTERIZATION AND MODELING

Wireless transmission channel is modeled as a random, time-varying system. The random nature of the channel is due to the fading process that causes variations in the received signal power. Those random variations arise from the Rayleigh (main cause) and shadowing fading experienced by the signal due to the multipath effect [14]. The time-variation characteristic of the channel comes from the different number of paths, attenuations, and delays. The impulse response of a time-varying channel will be a function of attenuations and time- and frequency delays. This means that both the time of arrival of the input pulse and the time passed since the arrival will influence on the channel model [2]. Several channel models exist. Here, will be presented the time-domain and the frequency-domain characterization.

The time-domain characterization represents the channel output as a series of weighted discrete delayed versions of the input signal. $L(n)$ paths are presented each associated with a different attenuation and different time and frequency delays. Thus the channel impulse response is given by

$$h(n, k) = \sum_{l=0}^{L(n)-1} \alpha_l(n) \delta(k - N_l(n)) e^{j\psi_l(n)n}, \quad (2.3)$$

where $\alpha_l(n)$ is the l^{th} propagation path gain, $N_l(n)$ is the l^{th} propagation delay and $\psi_l(n)$ is the Doppler effect. Parameters $\alpha_l(n)$ and $N_l(n)$ determine if the channel is slow or fast

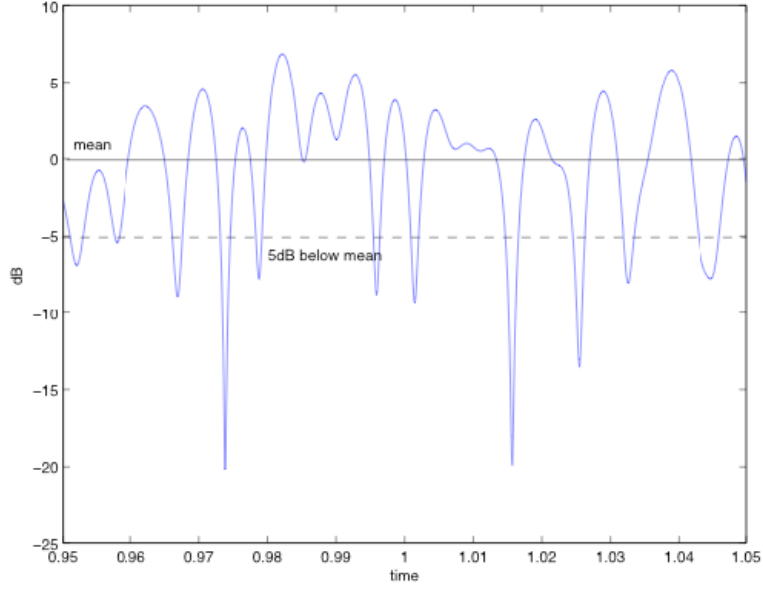


Figure 11: Time variation of the channel

varying [2]. Assuming that the parameters L , α , N_l and ψ are constant within a sent message, equation 2.3 can be written as

$$h(n, k) = \sum_{l=0}^{L-1} \alpha_l \delta(k - N_l) e^{j\psi_l n}, \quad 0 \leq n \leq N - 1. \quad (2.4)$$

On the other hand, the time-frequency characterization represents the channel output as a series of weighted discrete delayed and frequency shifted versions of the input signal.

$$H(n, \omega_k) = \sum_{l=0}^{L-1} \alpha_l e^{j\psi_l n} e^{-j\omega_k N_l},$$

which can be easily verified to be the Fourier Transform of the separable impulse response $h(n, k)$ in 2.4.

2.6 LMS FILTER

Adaptive filtering techniques have been used in many application areas such as signal prediction, system identification, noise cancellation, channel equalization and system inversion. In this work, the LMS adaptive filter is used to perform the bit detection.

An adaptive filter changes its performance based on the input signal. Some applications require adaptive coefficients since some parameters are not known in advance. For those applications, an adaptive filter, which uses a feedback loop to adjust the filter coefficients, may be the best choice. The adaptive filter adapts its coefficients according to the following equation:

$$W_{n+1} = W_n + \Delta W_n,$$

Where ΔW_n is the correction that is applied to the filter coefficients W_n at a time n for the set of new coefficients, W_{n+1} . Figure 12 shows a block diagram of an adaptive filter. The most important part of an adaptive filter is the set of rules, which describes how the coefficients are adapted (ΔW_n). According to [1], “Although is not yet clear what this correction should be, what is clear is that the sequence of corrections should decrease the mean-square error”.

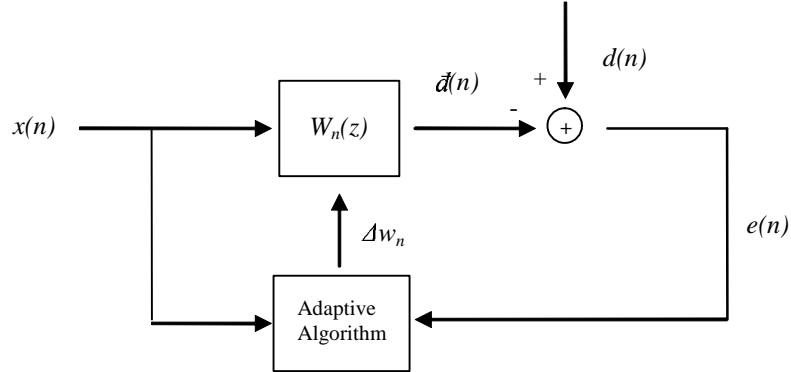


Figure 12: Block diagram of an adaptive filter

The adaptive filter should have the following properties:

- In a stationary environment, W_n sequences should converge to the solution of the Wiener-Hopf equations;
- The adaptive filter should calculate the estimation of the signal statistics $r_x(k)$ and $r_{dx}(k)$;
- In a non-stationary environment, the adaptive filter should be able to adapt to the changing statistics.

2.6.1 LMS Algorithm

There are two main different types of adaptive filter correction algorithms: The Least-Mean Square Algorithm (LMS Algorithm) and the Recursive Least Squares Algorithm (RLS Algorithm). The LMS algorithm is by far the most commonly used. In the LMS case, the goal is to find the coefficients W_n that minimizes the mean square error,

$$\xi(n) = E\{|e(n)|^2\},$$

The LMS uses the steepest descent algorithm to get the coefficients correction values. Since the steepest descent algorithm needs knowledge of the expectation $E\{e(n)x^*(n)\}$ and this value is generally unknown, an estimation of it is used. The estimation is given by:

$$E\{e(n)x^*(n)\} = \frac{1}{L} \sum_{l=0}^{L-1} e(n-l)x^*(n-l),$$

For the LMS algorithm case, $L = 1$ and a one-point sample mean is used. Therefore, the estimation equation is given by:

$$E\{e(n)x^*(n)\} = e(n)x^*(n),$$

and the coefficient update law will be given by:

$$W_{n+1} = W_n + \mu e(n)x^*(n),$$

The step size μ affects the rate at which W_n is corrected. If the value of μ is very small, the adaptation will be performed in a very slow basis. However, a big value of μ can lead to unstable and unbounded W_n 's trajectories. Table 1 describes the basic LMS algorithm.

Table 1: The LMS Algorithm for p^{th} -order FIR adaptive filter

<i>Parameters:</i>	p , Filter order
	μ , Step size
<i>Initialization:</i>	$\mathbf{w}_0 = \mathbf{0}$
<i>Computation:</i>	For $n = 0, 1, 2, \dots$
	(a) $y(n) = \mathbf{w}_n^T \mathbf{x}(n)$
	(b) $e(n) = d(n) - \hat{n}$
	(c) $\mathbf{w}_{n+1} = \mathbf{w}_n + \mu e(n) \mathbf{x}^*(n)$

2.7 JAMMING SIGNALS

A jammer can be described as a transmitter that interferes with radio or radar transmissions by beaming spurious signals into an enemy's radio or radar system. The goal is to not allow communication among one group. An important question is how can someone at the receiver side, overcome the effects of intentional jamming and become able to recover a sent signal? One way to answer is through the white Gaussian noise channel.

The definition of white Gaussian noise says that it is a mathematical model which has infinite power, spread uniformly over all frequencies. Communication is possible since only the finite power noise components in the signal spectrum can affect the sent signal. That means if some signal coordinates are not affected by the jammer, reliable communication can occur. In [16], a classical theory suggests the following design approach as a way to combat intentional jamming:

“Select signal coordinates such that the jammer cannot achieve large jammer-to-signal power ratio in these coordinates.”

If many different signal coordinates are available to send a signal, but only a small set of them are used and the jammer does not know which are them, two different situations can occur:

1. The jammer is forced to jam all frequencies with little power in each one.
2. The jammer is forced to jam some frequencies with more power than others.

So it is easy to verify that depending on how many different frequencies one has, more difficult it will be for someone to jam the signal. The number of signal coordinates are a function of the symbol period(T) and the bandwidth (W). If the period is fixed, the only way to increase the number is increasing the bandwidth which can be done by using spread spectrum.

It is assumed that the jammer does not have information about the synchronized spreading sequence. Even if the jammer gets a copy of one receiver, it will not be able to detect the synchronism of the spreading sequence. According to [16], *“the jammer has complete knowledge of the spread-spectrum system design except he does not have the key to the pseudorandom sequence generators.”*

2.7.1 Jammer Waveforms

There are different types of jamming waveforms. Intentional jamming signal has more variations than the additive Gaussian white noise which is assumed in conventional communications systems. In [16], an important statement is made:

“There is no single waveform that it is worst for all spread spectrum systems and there is no single spread-spectrum system that is best against all jamming waveforms.”

The structure of the most effective anti-jamming signals vary according to type of useful modulation, its parameters and type of demodulator [17].

2.7.1.1 Broadband and Partial-Band Noise Jammers A broadband noise jammer spreads Gaussian noise over the entire bandwidth with a total power J (Figure 13). The power is equally distributed over the total frequency range. Therefore, the jamming power spectral density is given by

$$N_j = \frac{J}{W},$$

The broadband jammer does not exploit any information about the anti-jam communication system besides its bandwidth. Hence it is a *brute force* jammer. It can be considered the

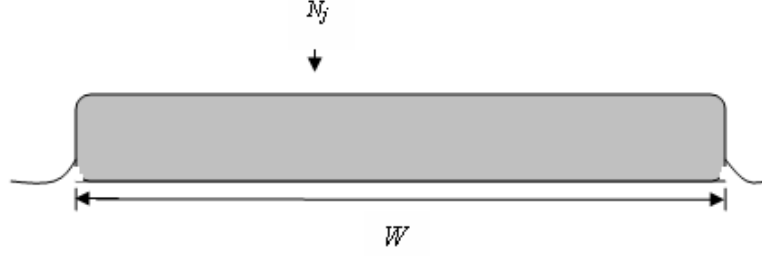


Figure 13: Broadband jammer in frequency domain

same as a white Gaussian noise with spectral density equal to N_j . A partial-band noise jammer (Figure 14), spreads noise of power J over a bandwidth W_j , where $W_j < W$.

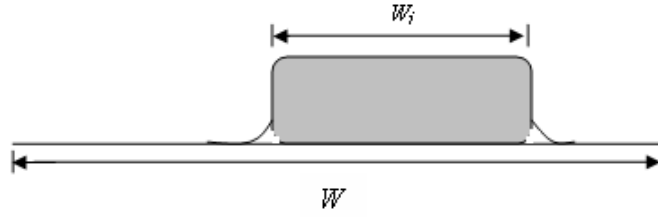


Figure 14: Partial jammer in frequency domain

2.7.1.2 Continuous Wave and Multitone Jammers When a jammer is only transmitting a steady carrier, this is referred to as *continuous wave* (CW) jamming. A CW jammer has the form

$$J(t) = \sqrt{2J} \cos[\omega t + \theta],$$

where θ is the random phase, ω is the frequency. The CW jammer introduces a bias with a constant amplitude but varying phase due to the frequency offset [18].

A combination of CW jammers is known as *multitone jammer* (MTJ). A MTJ is described by the following equation

$$J(t) = \sum_{l=1}^{N_t} \sqrt{2J/N_t} \cos[\omega_l t + \theta_l],$$

where N_t is the number of CW jammers and θ_l is each jammer phase. All phases are independent and uniformly distributed over $[0, 2\pi]$ and the total power J . According to Simon [19], the jammer's best strategy is to distribute the power J into N_t random phase tones which are contiguous and spaced in frequency by the symbol duration rate and vary the value of N_t to maximize the probability of error. Figures 15 and 16 show a CW and a MTJ in frequency domain respectively.

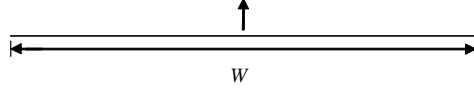


Figure 15: CW jammer in frequency domain

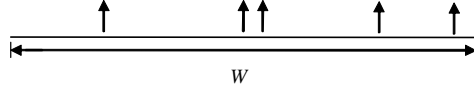


Figure 16: Multitone Jammer in frequency domain

2.7.1.3 Pulse Jammer A broadband pulse noise jammer transmits noise whose power is spread over the entire system bandwidth. However, the transmission only occurs for a fraction ϱ of the time. So one can say that ϱ is the duty cycle of the jammer transmission and $0 < \varrho \leq 1$. This allows the jammer to transmit with a power of

$$J_{peak} = \frac{J}{\varrho},$$

where J is the time-averaged power. The pulse jammer is very effective against spread-spectrum sequences [20].

2.7.1.4 Chirp Jammer A chirp jammer can be either partial or broadband jammer. It displays changing amplitudes and phases at different frequencies. Figure 17 shows time-domain representation of a chirp jammer

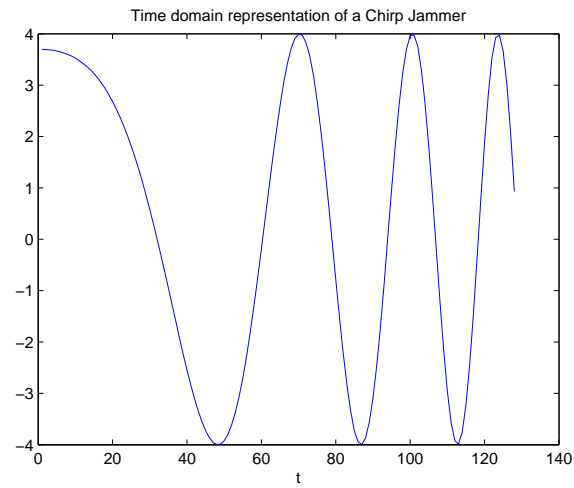


Figure 17: Chirp jammer in time-domain

3.0 CHANNEL ADAPTIVE ESTIMATION IN MC-SS

A *multi-carrier spread spectrum* (MC-SS) transmitting signal has an almost rectangular shape spectrum but its time-domain representation does not have a constant amplitude. This property is due to the IDFT transform and causes distortion when the signal is passed through a nonlinear power amplifier. Tan and Stuber [13] propose a spreading function that has a constant envelope both in time and in frequency domain. The function, a complex linear chirp of unit magnitude, is named *Complex Quadratic Sequences* and it is given by

$$\begin{aligned} g(n) &= e^{-j\frac{\pi}{8}} e^{j\frac{2\pi n^2}{N^2}} \quad , \quad n = 0, \dots, N-1 \\ G(k) &= e^{j\frac{\pi}{8}} e^{-j\frac{2\pi k^2}{N^2}} \quad , \quad k = 0, \dots, K-1 \end{aligned}$$

These sequences have some important properties [21]

- $g(n)$ and $G(k)$ are DFT pairs and $G(k) = g(k)^*$, where $*$ means complex conjugate,
- Circularly shifted versions of $g(n)$ and $G(k)$ are orthogonal,
- $g(n)$ and $G(k)$ have constant envelope.

In this work, the $g(n)$ and $G(k)$ functions are used as the spreading functions for the sent message. The use of such sequences simplifies the channel estimation and jammer detection process.

3.1 CHANNEL MODEL

In the time-domain, the baseband transmitted signal of an MC-SS is given by

$$\begin{aligned} s(n) &= \sum_{k=0}^{N-1} dG(k)e^{j\omega_k n}, \\ &= dg(n), \end{aligned}$$

where d is the data symbol $\{1, -1\}$ and $g(n)$ is the spreading sequence. Figure 18 describes a MC-SS transmitter. The sequence $s(n)$ is then sent throughout the channel which is

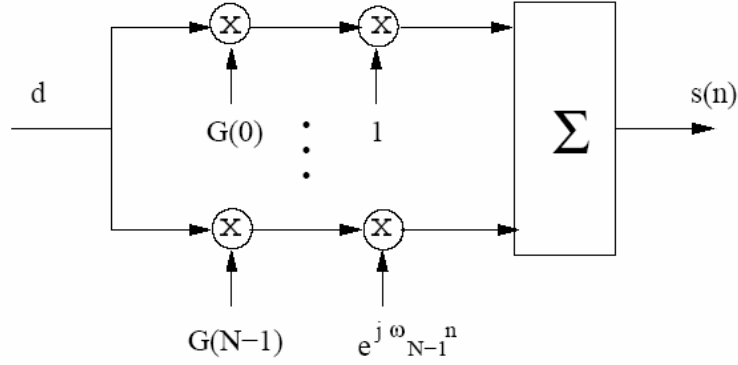


Figure 18: Multicarrier spread spectrum

characterized by delays, Doppler effect and attenuations. The channel output is given by

$$y(n) = d \sum_{l=0}^{L(n)-1} \alpha_l(n) g(n - N_l(n)) e^{j\psi_l(n)n}, \quad (3.1)$$

where $L(n)$ is the random number of paths, and $\alpha_l(n)$, $N_l(n)$, $\psi_l(n)$ are the attenuation, the time shift and the Doppler shift for each path. Therefore the channel is modeled as a random time-varying system. Assuming that the parameters $\{\alpha_l, N_l, \psi_l, L\}$ are constant for $0 \leq n \leq N - 1$. Equation 3.1 can be rewritten as

$$y(n) = d \sum_{l=0}^{L-1} \alpha_l g(n - N_l) e^{j\psi_l n},$$

The received signal, $r(n)$, is given by (time-domain representation)

$$r(n) = d \sum_{l=0}^{L-1} \alpha_l g(n - N_l) e^{j\psi_l n} + j(n) + \eta(n), \quad (3.2)$$

where $j(n)$ are the jammers and $\eta(n)$ is *additive white Gaussian noise* (AWGN). We consider three different types of jammers [16]. One creates a partial-band jammer composed of random sinusoids appearing together or separately in a frequency band. The second type generates a pulse-jammer that intermittently jams the whole transmission bandwidth by producing a random noise that appears as pulses. Finally, the third one creates a chirp-jammer capable of jamming a band of frequencies or most of the band, while displaying changing amplitudes and phases at different frequencies.

The representation of the received signal at a sub-channel k , $r_k(n)$ is

$$r_k(n) = [dG(k)H(n, e^{j\omega_k}) + j_k + \eta_k] e^{j\omega_k n}, \quad (3.3)$$

where j_k and η_k are respectively the jammer and noise component for each frequency k and

$$H(n, \omega_k) = \sum_{l=0}^{L-1} \alpha_l e^{-j\omega_k N_l} e^{j\psi_l n}, \quad (3.4)$$

is the frequency response of the channel. Since 3.3 is the received signal for each frequency k , one can obtain $r(n)$ in the following way

$$r(n) = \sum_k r_k(n),$$

Replacing 3.4 in 3.3 one gets

$$r_k(n) = [dG(k) \sum_{l=0}^{L-1} \alpha_l e^{-j\omega_k N_l} e^{j\psi_l n} + j_k + \eta_k] e^{j\omega_k n},$$

Figure 19 shows a frequency sub-channel.

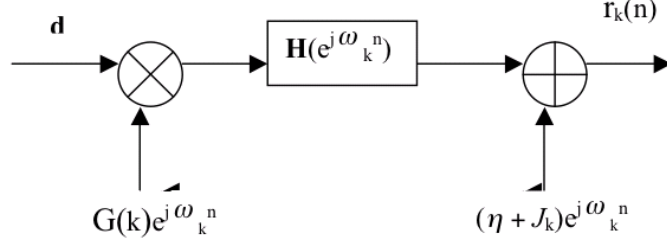


Figure 19: MC-SS frequency sub-channel

3.2 JAMMER DETECTION

The jammer detection is performed using the joint time-frequency *discrete evolutionary transform* (DET) [22] of the received signal $r(n)$, as well as its time and frequency marginals. The frequency marginal provides the frequencies where jammers occur, and determines the relation between the energies of the jammed received signal and the transmitted signals at each sub-channel. For a non-stationary received signal $r_k(n)$, the DET has a kernel

$$R(n, \omega_k) = \sum_l r(l)W(n, l)e^{-j\omega_k l}$$

where $W(n, l)$ is a time and frequency dependent window obtained from the Gabor or Malvar signal representation [22]. The evolutionary spectrum corresponding to $r(n)$ is given by $|R(n, \omega_k)|^2$. It is important to indicate that the DET is one of the few time-frequency methods where besides the non-stationary spectrum the signal has a representation based on the evolutionary kernel. The time and frequency-marginals corresponding to the signal are defined as

$$TM(n) = \sum_k |R(n, \omega_k)|^2 \quad , \quad FM(k) = \sum_n |R(n, \omega_k)|^2$$

The evolutionary spectrum combined with the time and frequency-marginals provide the information about the localization of the jammers in joint time-frequency, and separately in time or frequency. In order to detect the jammers, we compute the DET of $r(n)$, and compare its frequency marginals to the frequency marginals of the transmitted signal $s(n) = dg(n)$. If it is above a pre-defined threshold, a jammer is assumed to be present at that particular frequency. Figure 20 shows an example of a DET analysis of a signal jammed by 3 sinusoids, a pulse and a chirp jammer.

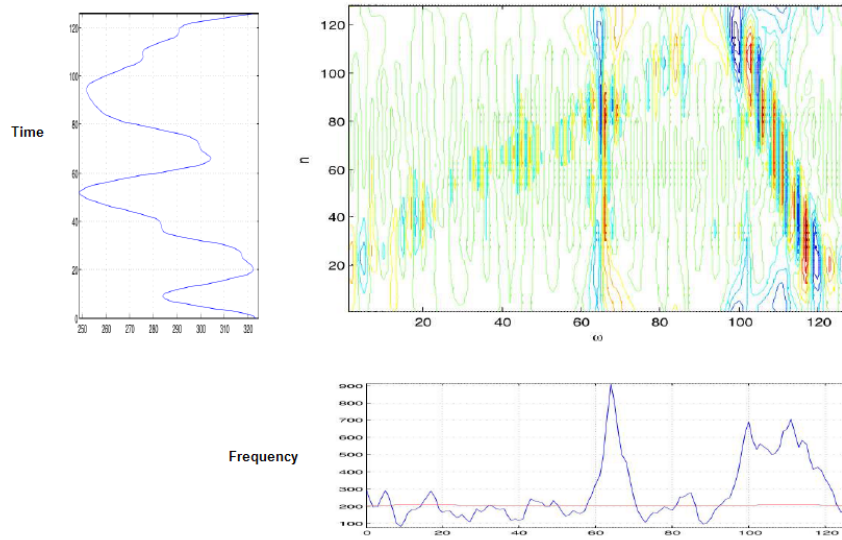


Figure 20: Time-Frequency Analysis

The figure on the bottom represents the frequency marginal and the threshold is shown as a continuous line. The idea is to mark those frequencies where supposedly a jammer is present. The big figure on the top, shows the time-frequency representation, and it can be clearly seen the shape of the linear chirp spreading function $g(n)$, the chirp jammer (on the right side), and one of the sinusoids. Since the sinusoids amplitude values are random, the other two are not clear in the figure but are present at $\omega = 100$ and $\omega = 110$.

3.3 CHANNEL ESTIMATION

According to equation 3.1 the channel is modeled as a random time-varying system. In [21], the following important characteristics of the spreading function $g(n)$ are shown.

1. Delay by N_0 :

$$\begin{aligned} g(n - N_0) &= e^{-j\frac{\pi}{8}} e^{j\frac{2\pi}{2N}(n-N_0)^2}, \\ &= g(n) e^{-j\frac{2\pi}{N}N_0n} e^{j\frac{\pi}{N}N_0^2}, \end{aligned}$$

where $e^{-j\frac{2\pi}{N}N_0n}$ corresponds to a Doppler shift $\psi_0 = \frac{-2\pi N_0}{N}$ and $e^{j(\frac{2\pi N_0^2}{2N})}$ is a constant.

2. Doppler frequency shift $\psi_1 = \frac{2\pi}{N}N_1$

$$\begin{aligned} g(n) e^{j\psi_1 n} &= e^{-j\frac{\pi}{8}} e^{j\frac{2\pi}{2N}n^2} e^{j\psi_1 n}, \\ &= g(n + N_1) e^{j\frac{2\pi}{2N}N_1^2}, \end{aligned}$$

where $g(n + N_1)$ is the spreading function $g(n)$ shift by N_1 samples (advanced) and $e^{-j(\frac{2\pi N_1^2}{2N})}$ is a constant.

3. Delay N_0 and Doppler frequency shift $\psi_1 = \frac{2\pi}{N}N_1$

$$\begin{aligned} g(n - N_0) e^{j\psi_1 n} &= g(n) e^{-j\frac{2\pi(N_0 - N_1)n}{N}} e^{j\frac{\pi N_0^2}{N}}, \\ &= g(n - N_0 + N_1) e^{-j\frac{\pi(N_1^2 - 2N_0N_1)}{N}}, \end{aligned}$$

the third item shows that if $g(n)$ is delayed in time by N_0 and shifted in frequency by $e^{j\frac{2\pi N_1}{N}n}$, the result will be a shift in time by an value $N_e = -N_0 + N_1$ and a multiplication by a complex factor. This characteristic allows to write the delay N_e and the Doppler ψ_l as one shift $N_{e,l}$.

Based on this, the channel response can be rewritten as

$$y(n) = \sum_{l=0}^{L-1} \alpha_l g(n - N_{e,l}),$$

where $N_{e,l}$ represents the time-delay and the Doppler effect. The estimation of the channel is simplified because now the channel can be considered as a *linear time-invariant* (LTI) system and its estimation consists in finding the equivalent time shifts [21].

The method described in [23] is used to perform the channel estimation. The LTI nature of the model, due to the use of the spreading sequence $g(n)$ [13], simplifies the calculation of the estimate since both delay and Doppler effects can be described as a time shift.

The transfer function of the channel is given by

$$H(z) = \sum_{l=0}^{L-1} \alpha_l z^{-N_{e,l}},$$

and the impulse response is

$$\tilde{h}(n) = \sum_{l=0}^{L-1} \alpha_l \delta(n - N_{e,l}),$$

3.3.1 Multipath Estimation using Discrete Evolutionary Transform (DET)

The time energy density and the frequency energy density do not completely describe what is happening with a time-varying signal. Therefore, a combined approach, looking at the time and the frequency domain at the same time can bring more information about the signal. There are four main reasons to use time-frequency analysis [24]

- Frequency analysis allows to learn something about the source.
- Propagation of waves through a medium generally depends on frequency
- It simplifies the understanding of the waveform
- Fourier analysis is a powerful tool for the solutions of ordinary and partial differential equations

From the frequency magnitude spectrum, it is possible to find out which frequencies were present, but there is no information about when those frequencies existed. Therefore, it is necessary to describe how the frequency spectrum is changing in time. The time-frequency approach is very useful in understanding the time-varying systems. "The difference between the spectrum and a joint-time frequency representation is that the spectrum allows us to determine which frequencies existed, but a combined time-frequency analysis allows us to determine which frequencies existed at a particular time" [24]

Due to its characteristics, a joint time-frequency representation is suitable for a non-stationary signal analysis. In this work, the method chosen to perform a time-frequency representation was the *Discrete Evolutionary Transform* (DET) [22].

DET is calculated by expressing the kernel $Y(n, \omega_k)$ in terms of the non-stationary received signal $y(n)$, for $0 \leq n \leq N - 1$. Gabor and Malvar [22] signal representations are used to express the kernel. The evolutionary kernel of $y(n)$ is expressed by

$$Y(n, \omega_k) = \sum_{m=0}^{N-1} y(m) W_k(n, m) e^{-j\omega_k m}, \quad 0 \leq k \leq K - 1,$$

where $W_k(n, m)$ is a time-frequency dependent window obtained from Gabor or Malvar signal representation. This representation is not suitable for our application, since we need to consider a signal-dependent window that can be adapted to the Doppler frequencies of the channel [23]. Considering that neither jammer nor noise are present, the output of a LTV channel is given by

$$\begin{aligned} y(n) &= \sum_{k=0}^{N-1} dG(k) \left[\sum_{l=0}^{L-1} \alpha_l e^{j\psi_l n} e^{-j\omega_k N_l} \right] e^{j\omega_k n}, \\ &= \sum_{k=0}^{N-1} Y(n, \omega_k) e^{j\omega_k n}, \end{aligned}$$

where

$$H(n, \omega_k) = \sum_{l=0}^{L-1} \alpha_l e^{j\psi_l n} e^{-j\omega_k N_l},$$

is the frequency response of the LTV channel. The evolutionary kernel is given by

$$Y(n, \omega_k) = \sum_{l=0}^{L-1} \alpha_l e^{j\psi_l n} e^{-j\omega_k N_l} dG(k),$$

and the frequency response of the channel can be calculated as a function of the evolutionary kernel and the spread function

$$H(n, \omega_k) = \frac{Y(n, \omega_k)}{dG(k)},$$

The bifrequency function $B(\Omega, \omega_k)$ is calculated by performing the DFT of $H(n, \omega_k)$ with respect to the n variable:

$$B(\Omega, \omega_k) = 2\pi \sum_{l=0}^{L-1} \alpha_l e^{-j\omega N_l} \delta(\Omega - \psi_l),$$

and calculating the inverse DFT of $B(\Omega, \omega)$ with respect to ω we find the spreading function

$$S(\Omega, k) = 2\pi \sum_{l=0}^{L-1} \alpha_l \delta(\Omega - \psi_l) \delta(k - N_l),$$

which displays peaks located at the delays and the corresponding Doppler frequencies having $2\pi\alpha_l$ as their amplitudes [2]. Using the properties of the sequence $g(n)$, the channel estimation as said before, is simplified. Replacing the effects of the time and the Doppler shifts by the effective time shifts allows to use the evolutionary kernel and the frequency response of the LTI channel independent of n .

$$Y(0, \omega_k) = \sum_{l=0}^{L-1} \alpha_l e^{-j\omega_k N_{e,l}} dG(k), \quad H(0, \omega_k) = \sum_{l=0}^{L-1} \alpha_l e^{-j\omega_k N_{e,l}},$$

the spreading function is also independent of Ω

$$S(0, m) = 2\pi \sum_{l=0}^{L-1} \alpha_l \delta(m - N_{e,l}),$$

In fact, \tilde{h} in 3.5 coincides with $S(0, n)$ [21]. If noise and/or jammer are present in relatively low power, the effective shifts $N_{e,l}$ are only estimates, but still can be used to detect the sent bit d . In this work, since the jammer power level can be extremely high, we developed an adaptation that reduces the amount of jammer allowing the channel estimation to work properly.

3.4 ADAPTATION FOR CHANNEL ESTIMATION

Assuming that jammers significantly affect the signal in some of the sub-channels it is necessary to adapt the received signal $r_k(n)$ before performing the channel estimation. The procedure is based on the frequency characterization of the received signal and it is used as a way to minimize the effects of the jammers.

The received signal is given by equation 3.3. After the jammer detection is performed the sub-channels where jammers are present become known. A function p_k is introduced to indicate whether a jammer is present ($p_k = 1$) or not ($p_k = 0$), the jammer detection process was described previously in section 3.2. Inserting p_k in equation 3.3 we get

$$r_k(n) = [dG(k)H(e^{j\omega_k}) + p_k J_k + \eta_k]e^{j\omega_k n}, \quad (3.5)$$

Given the possible concentration of the jammer at certain frequencies, the J_k component could be large and capable of overpowering the useful data at those frequencies. In this work, we assume that when a jammer is present it overpowers the sent signal. Based on that assumption, a new value for $r_k(n)$ is used for those frequencies containing jammer. The goal here is to minimize the jammer effect improving the channel estimation process. Basically the output, $r_k(n)$, at those sub-channels is changed. To effect this we replace these $r_k(n)$ by

$$\hat{r}_k(n) = \frac{r_k(n)e^{j\angle G(k)}}{|r_k(n)|}, \quad (3.6)$$

here, it is assumed that since a jammer is present, the received information is not reliable anymore. Values of $G(k)$ are known by the receiver. Considering that the jammer overpower the whole received signal, i.e.

$$r_k(n) \approx J_k,$$

Replacing the approximated value of $r_k(n)$ in 3.6 one gets

$$\hat{r}_k(n) = \frac{J_k e^{j\angle G(k)}}{|J_k|},$$

however, $J_k = |J_k|e^{j\angle J_k}$, and $|G(k)| = 1$ (properties of the spreading function $G(k)$ for all values of k)

$$\begin{aligned}\hat{r}_k(n) &= \frac{|J_k|e^{j\angle J_k}e^{j\angle G(k)}}{|J_k|}, \\ &= |d|G(k)e^{j\angle J_k}e^{j\angle G(k)},\end{aligned}$$

Adding the rest of the frequency components, we have a modified received signal $\hat{r}(n)$ that is suitable for the channel estimation as done in [21] and described previously in section 3.3. The channel estimation has as output for each data symbol the number of paths L , attenuations α_l and the effective time delays $N_{e,l}$ for each path. Those values are used as an input to the adaptive filter that performs the bit detection.

3.5 BIT DETECTION

An LMS adaptive filter is used to perform the bit detection. Two different methods are used, one uses the frequency-domain, while the other one uses the time-domain. In the frequency and in the time domain approach the bit detection is done in two different ways. The first one does not perform a channel estimation, therefore the LMS detects the sent bit without any prior information about the channel. The second one uses the results obtained from the channel estimation step as an initial value for the adaptive filter's coefficients. Figure 21 shows the model used.

The first method to be introduced uses the frequency representation of the received signal $r_k(n)$. The bit detection is performed after the jammer detection (described in section 3.2), therefore it is possible to choose a frequency where no jammer component is present (meaning $p_k = 0$).

The time domain method uses the received signal in the time domain, $r(n)$, to detect the sent bit. As done in the frequency domain method, an LMS filter is responsible for the bit detection and two the same two approaches are taken (with and without channel estimation). The estimation method is described in section 3.3. In both methods (time and frequency domain), two different values are used as a reference value; 1 and -1.

The bit detection is based on the reference value that has the smallest error E . The following sections will describe the procedure for each of the methods here introduced.

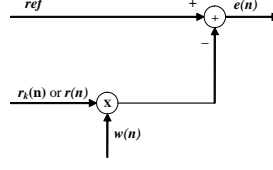


Figure 21: Model of LMS adaptive filter

3.5.1 Frequency-Domain Bit Detection without Channel Estimation

The first method to be described is the frequency-domain detection with no channel estimation. This procedure uses as an initial filter coefficients only the conjugate complex value $G^*(k)e^{-j\omega_k n}$. That means no other information besides the spreading function and the received signal is given to the receiver. Thus $w_0(n)$ (initial filter coefficients) is given by

$$w_0(n) = G(k)^* e^{-j\frac{2\pi kn}{N}},$$

w_0 is the same for both reference values. The initial error vector for each reference value is given by

$$\begin{aligned} e(n) &= ref - w_0(n)r_k(n), \\ &= ref - G(k)^* e^{-j\frac{2\pi kn}{N}} [dG(k)H(e^{j\omega_k}) + \eta_k] e^{j\omega_k n}, \end{aligned}$$

where ω_k is a frequency chosen accordingly to our jammer detection process and ref is the reference value used. It is assumed that $r_k(n)$ for this frequency k does not have a jammer component J_k since the function p_k is zero. The reference value, ref , is $\{1, -1\}$. Since $G(k)^*G(k) = 1$, the error vector can be written as

$$e(n) = ref - [dH(e^{j\omega_k}) + G(k)^*\eta_k],$$

where $e(n)$ changes after each LMS filter loop and $H(e^{j\omega_k})$ is given in 3.4. After the first iteration, the value of $e(n)$ is given by

$$e(n) = ref - w(n)r_k(n) \quad (3.7)$$

where w are the filter coefficients that minimizes the mean square error [1]. Those coefficients are updated as a function of the error $e(n)$ and the step parameter μ . Since $e(n)$ is calculated by 3.7, it is also updated every time that the value of w changes.

The error vector $e(n)$ is then calculated for each value of n , where $0 \leq n \leq N - 1$, and for each reference value. The result are two final error vectors $E_{ref1}(n)$ and $E_{ref2}(n)$, one for each reference value. A summation over time of the absolute value of $E_{ref1}(n)$ and $E_{ref2}(n)$ is then performed resulting in two values: E_{ref1} and E_{ref2} . Both values are then compared, and the smallest is chosen. Finally, since the errors are calculated based on the reference values (that are the same as the possible sent bits), the chosen reference value it is designated as the sent bit.

3.5.2 Frequency-Domain Bit Detection with Channel Estimation

The use of channel information as an input parameter for the LMS adaptive filter can improve the results. That assumption is tested in this thesis. Miller and Rainbolt in [25], say that “there is a substantial benefit to be gained by attempting to track all the fading process.” In this work, we use the time-frequency modeling to obtain information about the channel, tracking the fading.

The channel estimation process provides the delay-doppler ($N_{e,l}$), the number of paths (L) and the attenuation (α_l) for each path. Those parameters are used as a initial value for w_0 . The concept is the same used in the former case, the difference is that in the previous section no information about the channel is used as an input to the LMS filter. The w_0 is expressed in the same way as in 3.7 but with some information added. This information are the values found in the channel estimation process. Hence w_0 now is given by

$$w_0(n) = \frac{G(k)^* e^{-j\omega_k n} e^{j\frac{2\pi N_{e,0}}{N}}}{\alpha_0},$$

where $N_{e,0}$ corresponds to the closest signal (i.e., least attenuated) and α_0 its correspondent attenuation. Thus the value of $e(n)$ for the first iteration is

$$\begin{aligned} e(n) &= ref - \frac{G(k)^* e^{-\frac{j\omega_k n}{N}} e^{j\frac{2\pi k N_{e,0}}{N}} [dG(k)H(e^{j\omega_k}) + \eta_k] e^{j\omega_k n}}{\alpha_0}, \\ &= ref - \frac{[dH(e^{j\omega_k}) + \eta_k G(k)^*] e^{j\frac{2\pi k N_{e,0}}{N}}}{\alpha_0}, \end{aligned}$$

where $H(e^{j\omega_k})$ is given in 3.4. Finally, $e(n)$ is given by

$$e(n) = ref - \left[d + \frac{\sum_{l=1}^{L-1} \alpha_l e^{j\omega_k (N_{e,0} - N_l)} + \eta_k G(k)^* e^{j\frac{2\pi k N_{e,0}}{N}}}{\alpha_0} \right],$$

the value of $e(n)$ is updated after each change in the filter's coefficients values, $w(n)$. As done in the previous section, $e(n)$ is calculated for both reference values. Then, a summation over n of the absolute value of $e(n)$ is performed. As a result, one gets two scalars (one for each reference value) E_{ref1} and E_{ref2} . Following the same procedure as in section 1.5.1 we obtain the sent bit.

3.5.3 Time-Domain Bit Detection without Channel Estimation

The approach used in this section is in a certain way similar to the ones described before. The received signal, $r(n)$, and the reference values $\{-1, 1\}$ are used as a input for the LMS adaptive filter. The initial value for the filter coefficients, w_0 , again performs an important role in the bit detection.

Here, the initial condition will be a function of the conjugate of the spreading sequence $g(n)$. Therefore w_0 is given by

$$w_0(n) = g^*(n),$$

and the error vector $e(n)$, given that $r(n)$ is described by 3.2, is

$$\begin{aligned} e(n) &= ref - w_0(n)r(n), \\ &= ref - g^*(n) \left[d \sum_{l=0}^{L-1} \alpha_l g(n - N_l) e^{j\psi_l n} + j(n) + \eta(n) \right], \end{aligned}$$

the channel impulse response is given by

$$h(n) = \sum_{l=0}^{L-1} \alpha_l \delta(n - N_l) e^{j\psi_l n}$$

using the spreading sequence properties, the delay and the Doppler can be represented as joint shift

$$\tilde{h}(n) = \sum_{l=0}^{L-1} \alpha_l \delta(n - N_{e,l})$$

and the received signal, $r(n)$, can be rewritten as

$$r(n) = d \sum_{l=0}^{L-1} \alpha_l g(n - N_{e,l}) + j(n) + \eta(n)$$

the error vector now can be described as

$$e(n) = ref - \left\{ d \sum_{l=0}^{L-1} \alpha_l \delta(n - N_{e,l}) + g(n)^* [j(n) + \eta(n)] \right\}$$

The error vector is then updated as in equation 3.7 and it is calculated for each reference value, $\{1, -1\}$. The same procedure used in the previous sections is used for the time-domain bit detection, meaning that the reference that provides the smallest error E will be chosen as the sent bit.

3.5.4 Time-Domain Bit Detection with Channel Estimation

In this section we use the channel estimation results as a way to improve the performance of the bit detector. The estimation is the same as described in section 3.3. Thus the channel estimation provides the delay-Doppler ($N_{e,l}$), the number of paths (L) and the attenuation (α_l) for each path. Those values will be used as a part of w_0 . We use the delay-Doppler value, $N_{e,l}$, to shift the spreading function $g(n)$ in time. This means that instead of having a function $g(n)$, we will have a delayed version of the spreading function given by $g(n - N_{e,l})$. Considering that the channel estimation provides the information $N_{e,0}$ and α_0 (closest path, $l = 0$). As in the delay case, we will consider one attenuation value and we call it α_l . Hence, w_0 will be

$$w_0(n) = \frac{g(n - N_{e,0})^*}{\alpha_0}$$

here again $N_{e,0}$ is the closest signal (i.e., least attenuated) and α_0 its correspondent attenuation and the initial error vector is

$$\begin{aligned} e(n) &= ref - w_0(n)r(n), \\ &= ref - \frac{g(n - N_{e,l})^* [d \sum_{l=0}^{L-1} \alpha_l g(n - N_l) e^{j\psi_l n} + j(n) + \eta(n)]}{\alpha_0}, \end{aligned}$$

taking $l = 0$ out of the summation

$$e(n) = ref - g(n - N_{e,l})^* \left[d\alpha_0 g(n - N_0) e^{j\psi_0 n} + d \sum_{l=1}^{L-1} \alpha_l g(n - N_l) e^{j\psi_l n} + j(n) + \eta(n) \right] / \alpha_0,$$

however, the channel estimation represents both the delay and Doppler by the shift $N_{e,l}$ and according to the $g(n)$ properties that allow the analysis of the channel as a LTI [21], we consider a Doppler shift as a delay and the received signal can be written as

$$r(n) = d \sum_{l=0}^{L-1} \alpha_l g(n - N_{e,l})$$

Therefore the error is given by

$$\begin{aligned} e(n) &= ref - \left[d + dg(n - N_{e,l})^* \sum_{l=1}^{L-1} \alpha_l g(n - N_l) e^{j\psi_l n} + g(n - N_{e,l})^* (j(n) + \eta(n)) \right] / \alpha_0, \\ &= ref - [d + g(n - N_{e,l})^* (j(n) + \eta(n))] \end{aligned}$$

3.6 SIMULATIONS

In this section, the effectiveness of the proposed method to detect the sent bit is measured by the *bit error rate* (BER). A multipath free channel is considered with perfect synchronization at the receiver. We use $N = 101$ sub-channels and assume a 505kHz bandwidth, the frequency spacing between the sub-carriers is 5 khz. For each pair (JSR, SNR) we perform 10000 Monte Carlo simulations to obtain the BER.

To illustrate the performance of the proposed method, three different jammers are added to the output of the channel: a chirp jammer, a pulse jammer and 3 sinusoids each with a random frequency and amplitude. The *Jammer to Signal ratio* (JSR) ranges from -6dB to 2 dB. The channel is considered fast fading, meaning that its characteristics change at each bit sent, and it is modeled as a time-varying with 5 different paths. The time-delays and Doppler frequency shifts are randomly chosen. The multipath gains, α_l , are linearly related to the delays. We simulate using three different threshold levels for the Doppler shift. In the first case, no Doppler is considered. The second one considers a maximum Doppler shift of 0.001π and the last one considers a maximum Doppler shift of 0.01π . For comparison purpose, if a car is at 60 mph and the carrier frequency is 1 GHZ, the nomralized Doppler will be approximately 0.0001π . In all cases the Doppler shift is the same for all paths within one message period. Besides jammers, AWGN is added to the signal. The *Signal to Noise ratio* (SNR) values considered in our simulations range from $-5dB$ to $15dB$.

First, we perform the simulations using the frequency-domain method. Figure 22 shows the results of estimating the sent bit using jammer detection (with and without channel estimation) and without using jammer detection (meaning that we randomly pick a frequency to use in the bit detection). The jammer detection identifies the frequencies where a jammer is present. That information is used to adapt the received signal $r(n)$ (used in the channel estimation) and to avoid the adaptive filter to pick a jammed frequency (bit detection). Here when we say that no jammer detection is used we are only refering to the bit detection part. Both methods, time- and frequency-domain, always use the jammer detection and signal adaptation prior to the channel estimation.

It can be verified that when no jammer detection is performed, the receiver performs poorly. Also the use of channel estimation increases the receiver performance. We simulated using a JSR of -2 dB, Doppler of 0.001π and a variable value of SNR.

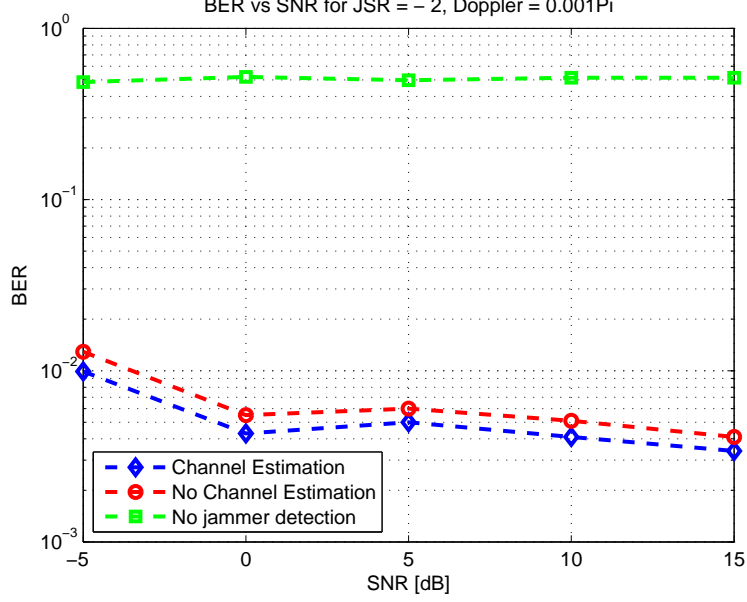


Figure 22: Comparison between approaches in the frequency-domain

The simulations results shown in Figs. 23, 24 and 25, are obtained using the frequency-domain approach with jammer detection and channel estimation for different Doppler values. As expected, the performance of the bit estimator degrades as the Doppler effect is increased although the performance is not significantly different when no Doppler is present and when a Doppler 0.001π is present. However when a higher Doppler value is used the estimator performance degrades enourmosly. This can be explained by the fact that the LMS filter does not adapt fast enough to counteract the Doppler effect [26].

The same simulations done in the frequency-domain are performed in the time-domain with the same values for SNR, JSR and Doppler. Initially, we consider wheter the jammer detection in the bit estimation part of the process improves or not the BER. It is important again to emphasize that jammer detection and adaptation of the received signal are performed for channel estimation in all simulations. Here, we are discussing the use of jammer detection only in the last part of the process that is the bit detection done by the LMS filter.

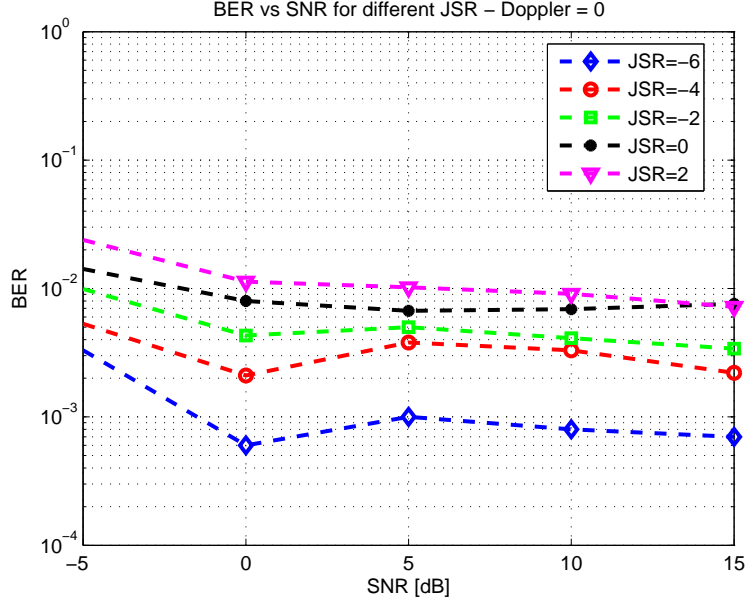


Figure 23: BER vs SNR frequency-domain without Doppler

Figure 26 shows that the use of jammer detection does not improve BER in the time-domain approach. Hence, we do not use the adapted version of the received signal $r(n)$ as a input to the adaptive filter but we still using the adapted version of the received signal to perform the channel estimation. In other words, the signal adaptation is used only in the first part (channel estimation), while in the bit detection (performed by the adaptive filter) the original received signal is used. The next step is to verify whether the channel estimation improves the results. Figure 27 shows a comparison between a bit estimation with and without channel estimation in the time-domain.

It can be verified that in the time-domain the channel estimation improves the results more than in the frequency-domain. In the time approach the BER is reduced 40% when using the channel estimation, while in the frequency-domain the reduction is only 17%. The use of jammer detection and signal adaptation prior to the channel estimation is important to assure that even with a high level of jammer the estimation can be done.

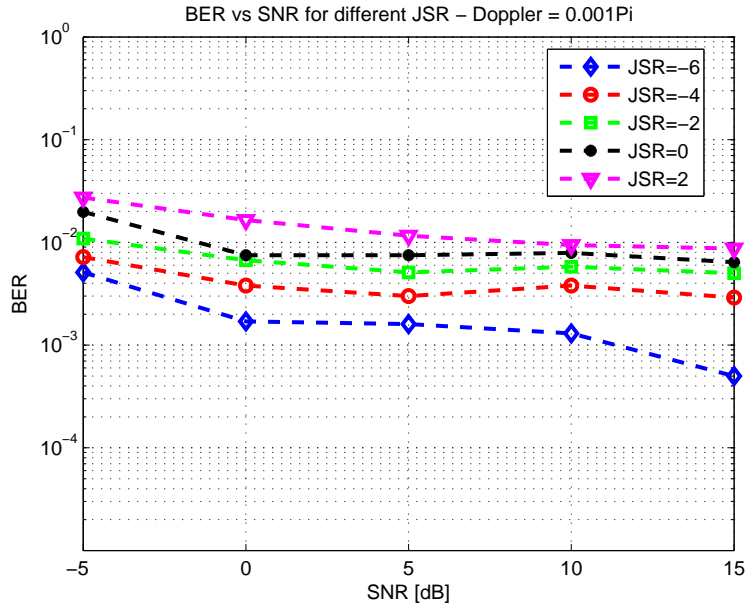


Figure 24: BER vs SNR frequency-domain with Doppler = 0.001π

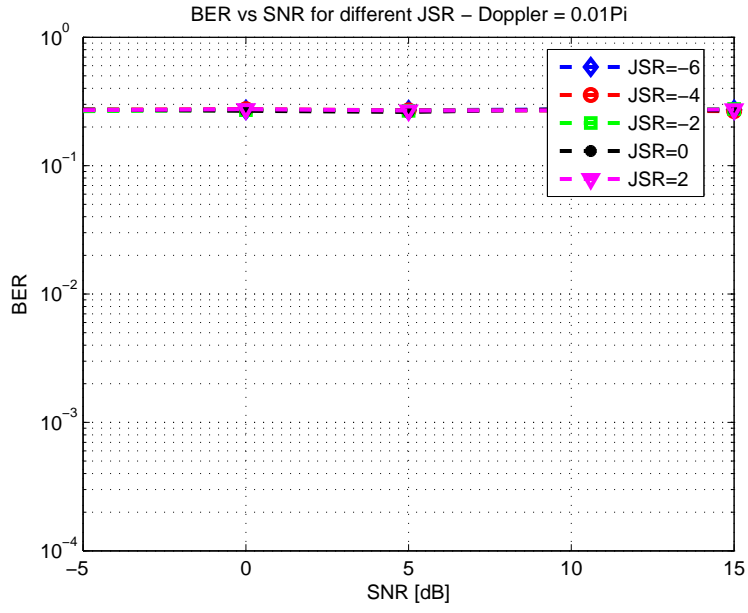


Figure 25: BER vs SNR frequency-domain with Doppler = 0.01π

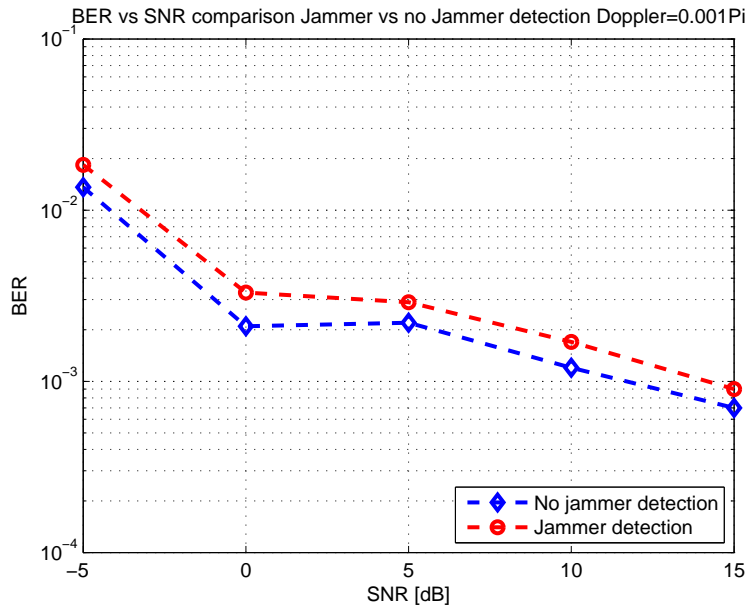


Figure 26: Comparison time-domain with and without jammer detection, JSR=0dB

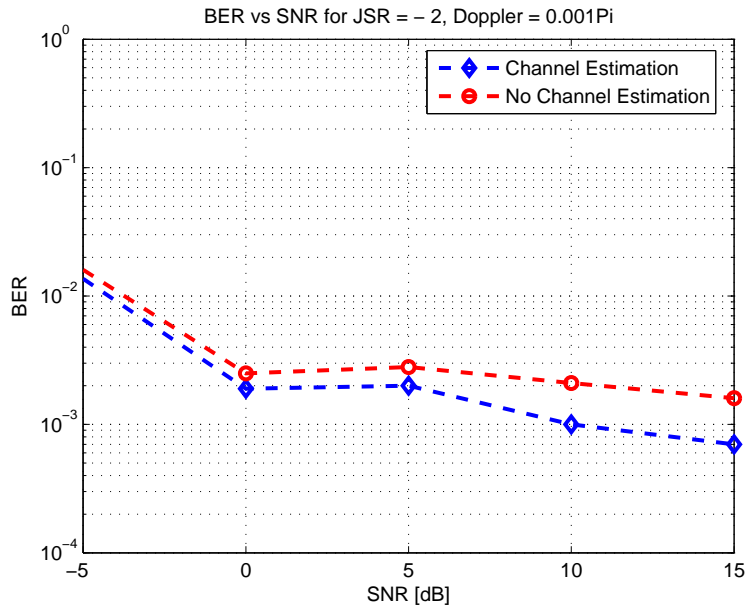


Figure 27: Comparison time-domain with and without channel estimation

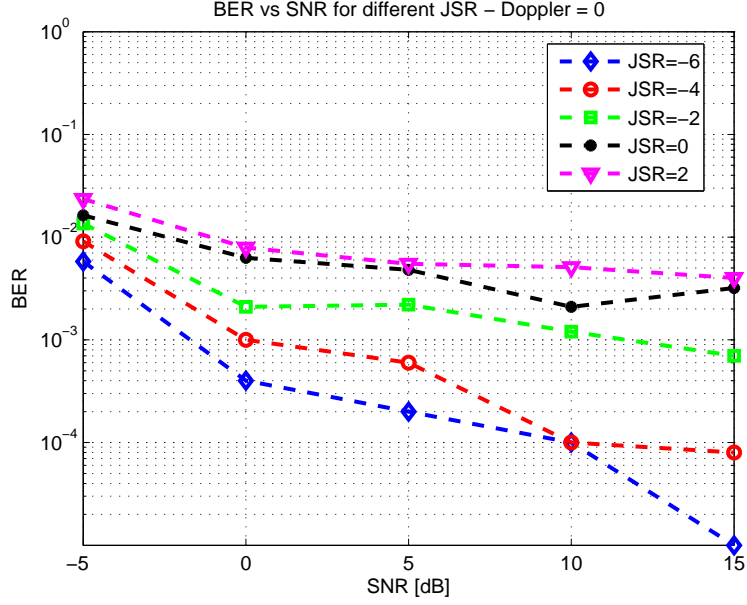


Figure 28: BER vs SNR time-domain without Doppler

Figures 28, 29 and 30 show the results of the time-domain approach. As done in the frequency-domain simulations, we estimate the bit for 3 different values of Doppler, and 5 values of SNR and JSR. Channel estimation was used for all simulations.

The time- and frequency-domain approaches present almost the same results for small values of Doppler while with a $\text{Doppler} = 0.01\pi$ the time-domain method achieves much better results (around 60% improvement). This improvement probably has to do with the redundancy present in the time-domain approach. This does not happen in the frequency domain because we choose only one channel where the bit estimation is performed. Figures 31 and 32 show a comparison between the time- and frequency-domain results.

In Figs. 33 and 34 flow charts are presented showing a macro view of the whole process. The first one shows the frequency-domain approach while the second one shows the time-domain approach.

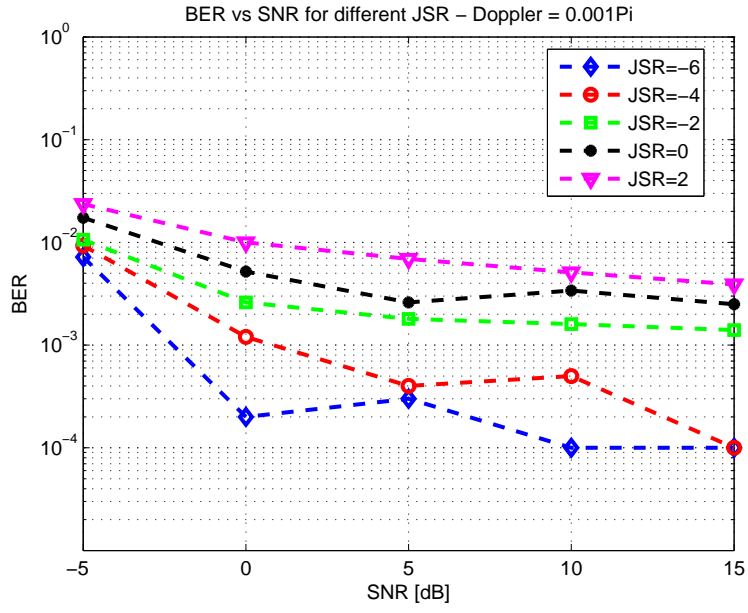


Figure 29: BER vs SNR time-domain with Doppler = 0.001π

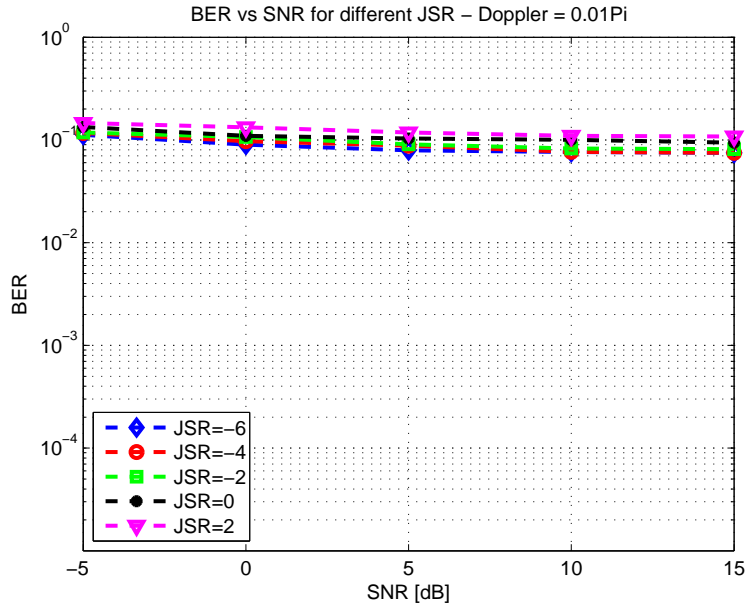


Figure 30: BER vs SNR time-domain with Doppler = 0.01π

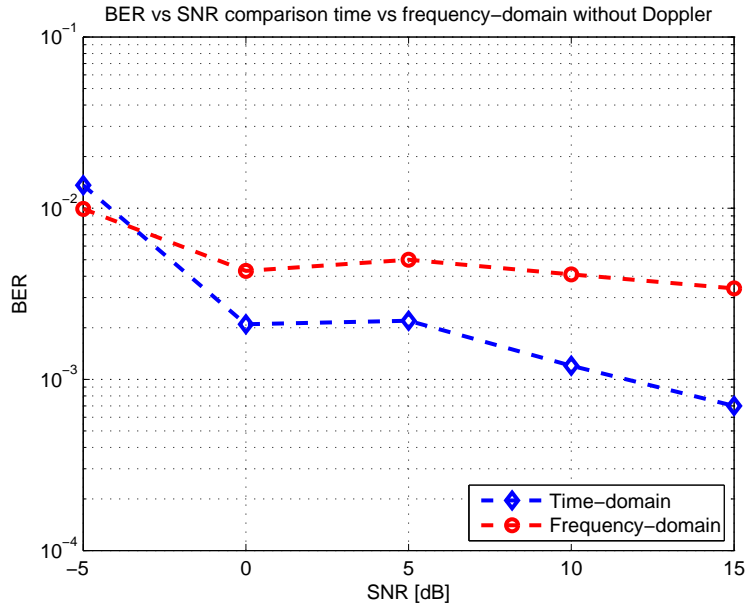


Figure 31: BER vs SNR time- vs frequency-domain without Doppler JSR=-2 dB

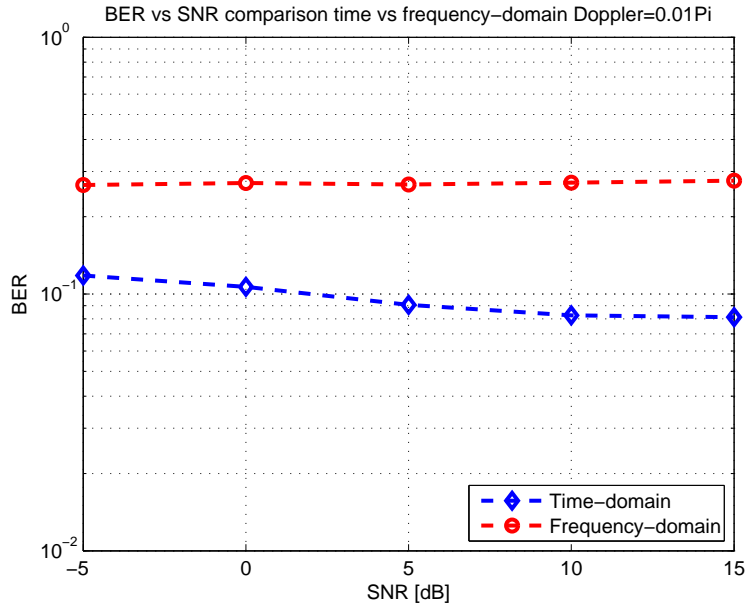


Figure 32: BER vs SNR time- vs frequency-domain with Doppler=0.01 π JSR=-2 dB

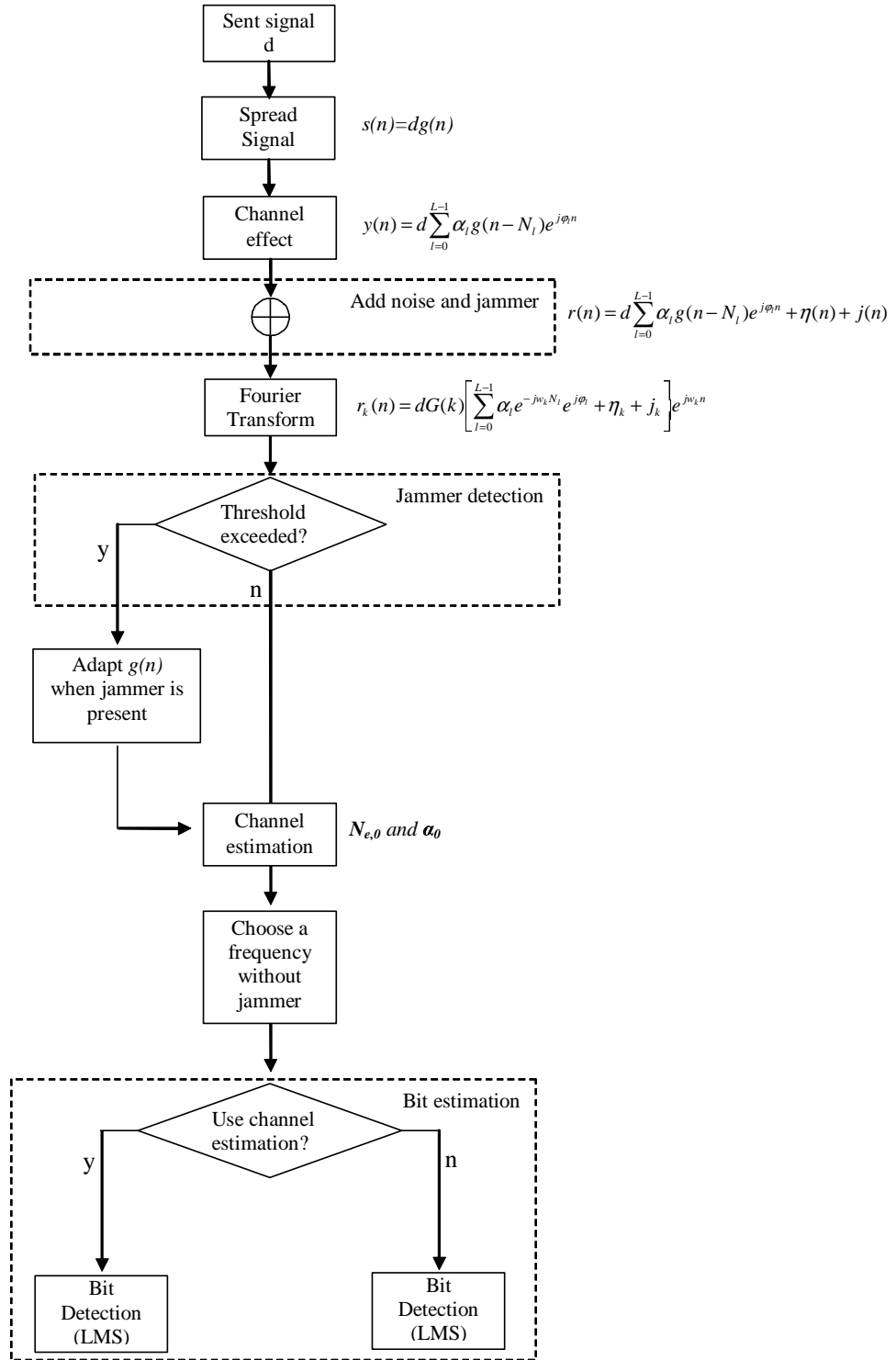


Figure 33: Algorithm frequency-domain detector flow chart

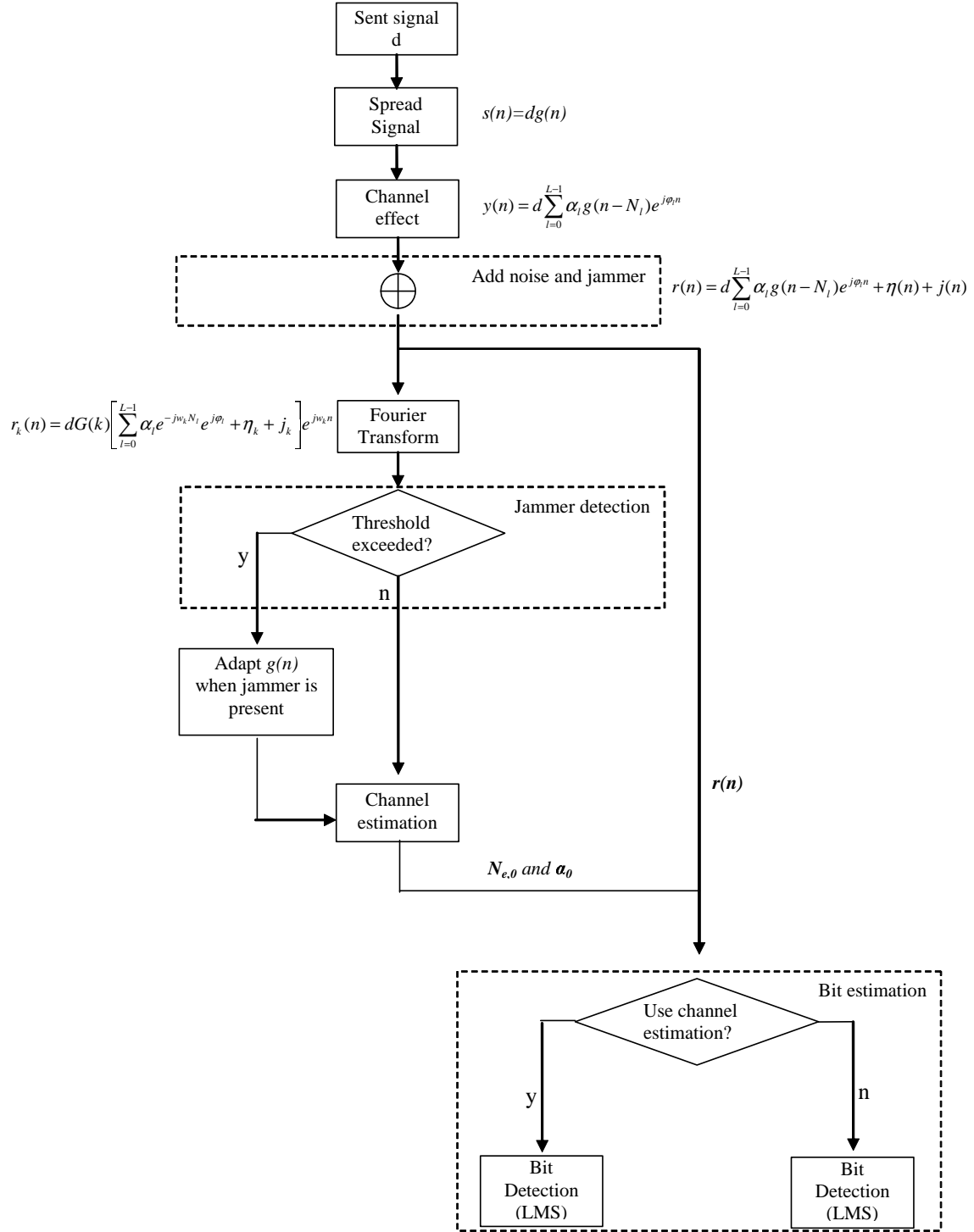


Figure 34: Algorithm time-domain detector flow chart

4.0 CONCLUSIONS

This dissertation addressed the problem of wireless transmission through a multipath communication channel in which additive white noise and jammers are present. The channel is characterized by its delays, gain attenuation and number of paths and it is a linear time-variant channel. We assume that the channel is constant over a single data symbol or frame transmission. This assumption plus the use of linear chirp sequences, allow us to consider the channel as a linear time-invariant for each sent message. Therefore the channel estimation process is easier to be executed.

The presence of jammers can affect the channel estimation, so an adaptation in the received signal might be necessary. To execute this adaptation, we used a jammer detector based on the time-frequency representation of the received signal to determine which frequencies are jammed. For the frequencies with a jammer component, a new value of $r_k(n)$ is calculated minimizing the jammer effects and allowing the channel estimation.

A time-frequency representation used to identify the frequencies where a jammer is present increases the bit estimation performance in the frequency-domain approach. This is due to the fact that an unaffected frequency is chosen to perform the estimation. The same results are not obtained in the time-domain method where the use of jammer detector does not improve the bit error rate.

The use of an adaptive filter to estimate the sent bit provides good BER even when a high JSR and SNR are present. However, the performance degrades when the Doppler component is big. This can be explained by the fact that the adaptive filter is not fast enough to track the received signal. This is a interesting issue to be addressed in future work.

4.1 FUTURE WORK

The problem of efficient bit estimation and channel estimation when both Doppler and time-delay are present in the wireless channel is still an area for further research. At present, this research focuses on modeling and estimation of multi-carrier spread spectrum communication channels only. The next step would be extend the methods used to other communications schemes such as OFDM.

One way of expanding this work to OFMD could be the use of Slepian sequences. Those sequences can be used to narrow the spectrum around some determined frequency. After narrowing the signal, the same approach used in this work in the frequency-domain would be applied to the OFDM system.

Another important aspect is the Doppler effect. It is clear that the Doppler seriously degrades the performance of the bit estimator. Therefore, developing a better way to keep track of the Doppler is important to assure good results in a mobile use.

APPENDIX

MATLAB CODE

```
clc;
clear all;
close all;
warning off;

Teto=28;% Maximum size of delay
% Value of N
N=128; %original 101
NT=N+Teto;
n=0:N-1;
s2=zeros(NT);

% Values of SNR and JNR
SNR=[-5 -2 0 5 15]; % SNR in dBs
JSR=[-6 -4 -2 0 2]; % JSR in dBs
ERRORGNnochannel=zeros(5,5);
ERRORJAMMER=zeros(5,5);
ERRORGN=zeros(5,5);
ERRORGN1nochannel=zeros(5,5);
ERRORGN1=zeros(5,5);
errorjammer=0;
erradogn1s=0;
erradogns=0;
erradogn1ns=0;
erradognns=0;
%load pn.mat
for snr=1:5 % Loop SNR
    SNR1=10^(SNR(snr)/10);

    for jsr=1:5 %Loop JSR
        JSR1=JSR(jsr);
```

```

for li=2:30 %This is the outer loop that give us the number of inte
%rations for each simulation (SNR and JNR)
JAMMEDNOISE=zeros(1,N); %"cleaning" JAMMEDNOISE variable
Se=0;
% Generating d
r=rand(1,1);
if r>=.5
    d=1;
else
    d=-1;
end

% Modulating signals in frequency (G) and in time (gn)
G=exp(i*pi/8)*exp(-i*(pi/N).*n.^2);
%G=G.*PN;
gn=ifft(G);gn=gn/gn(1);

% Transmitted signal
s=zeros(1,N);
s=d.*gn;

% Channel multi-path
f=0:NT-1;
s2(li,:)=s(N-Teto+1:N) s];% adding cyclic prefix
for nm=1:5
    delay(nm)=ceil((Teto-1)*rand(1,1));
    alpha(nm)=(N-delay(nm))/N;
end
doppler=rand();
doppler = [dop*0.01000*pi dop*0.01000*pi dop*0.01000*pi dop*0.0100*pi dop*0.0100*pi];
% doppler = [0 0 0 0 0];

% Create the multipath (5 paths)
r11(li,:)= alpha(1)*exp(i*doppler(1).*f).*[s2(li-1,NT-delay(1)+1:NT) s2(li,1:NT-delay(1))];
r12(li,:)= alpha(2)*exp(i*doppler(2).*f).*[s2(li-1,NT-delay(2)+1:NT) s2(li,1:NT-delay(2))];
r13(li,:)= alpha(3)*exp(i*doppler(3).*f).*[s2(li-1,NT-delay(3)+1:NT) s2(li,1:NT-delay(3))];
r14(li,:)= alpha(4)*exp(i*doppler(4).*f).*[s2(li-1,NT-delay(4)+1:NT) s2(li,1:NT-delay(4))];
r15(li,:)= alpha(5)*exp(i*doppler(5).*f).*[s2(li-1,NT-delay(5)+1:NT) s2(li,1:NT-delay(5))];
smulti(li,:)=r11(li,:)+r12(li,:)+r13(li,:)+r14(li,:)+r15(li,:);%Add up all my paths

% Generating channel noise with certain SNR
Se=var(s);
sigman=sqrt(Se/SNR1);
t=randn(1,NT);
vart=var(t);
t=t/sqrt(vart);
noise=sigman*t;

```

```

noise=noise-mean(noise);

%Setting and adding noise and jammers
A=1;          % Amplitude of the jammer signal
K=3;          % Number of exponential jammer (0 to 8)
chirp='y';    % Choose Y or N
pulse='y';    % Choose Y or N
Jammer(li,:)=jammer21(n,A,N+Teto,K,chirp,pulse); %Call the fun
%ction that generates the jammer and the noise
Je=Jammer(li,:)*transpose(conj(Jammer(li,:)));
Jammed129(li,:)=noise+smulti(li,:); %Without jammer, only noise
%and multipath
varjammer=var(s)*(10^(JSR(jsr)/10));
jamm=Jammer(li,:)*sqrt(abs(varjammer))/sqrt(abs(var(Jammer(li,:))));
%only to verify jammer signal
Jammed129(li,:)=Jammed129(li,:)+jamm;
% Frequency domain
Jammed(li,:)=Jammed129(li,Teto+1:NT);%cyclic prefix discarded
JAMMED(li,:)=fft(Jammed(li,:),N)/sqrt(N);%Jammed signal frequency domain

% Frequencies where possible jammers exist
Ja=abs(JAMMED(li,:));
Sa=abs(fft(s)/sqrt(N));
Mean=mean(Sa);

% This part looks for jammers
for k=1:N;
    if (Ja(k)>3.05*Mean) %Compare magnitude of S and magnitude
        %of JAMMED signal
        J(k)=1;
    else
        J(k)=0;
    end
end

% Frequencies where the threshold is exceeded
indices=find(J);
m=length(indices);
indicesnojammer=find(J==0);%Get the frequencies where we don't have jammer

% Applying the notch filter and multiplying received signal by g(n-no). This
% part gets rid of the noise. We create a new vector JAMMEDNOISE=JAMMED

JAMMEDNOISE=JAMMED(li,:);
JAMMEDNOISE(indices)=(JAMMED(li,indices)./Ja(indices)).*exp(j.*angle(G(indices)));

% This part gets rid of the jammer

```

```

% Generation of new gn sequence (gn1) with G at certain frequencies
G1=G;
G1(indices)=(JAMMED(li,indices)/Ja(indices)).*exp(j.*angle(G(indices)));
%Where is non-zero G will be set to zero to cancel the jammer
gntt=ifft(G1);
gntt=gntt/gntt(1);
gn1=conj(gntt);
sj=ifft(JAMMED(li,:)).*gn1;
% Getting rid of jammers
rec=ifft(JAMMEDNOISE); % Jammed signal in the time domain
REC=fft(rec,N)/sqrt(N); % Received signal in frequency domain
%after Jammer excision

% Decide if channel estimation is needed, use that if you just
% want to test something quickly
channelest='y';
if channelest=='y'

    % Call fucntion that will estimate the channel
    [SFF,H]= mcss_ch2(rec,REC,G);
    z=SFF(1,:);
    %%%THE IMPORTANT PART OF THE RECEIVER

    z21=z(1:51); %Question about this, he uses value 51 and 52,
    %probably has to do with N
    z22=z(52:101); %z21:shift on time axis due to delay
    %z22:shift on time axis due to Doppler
    x3=find(z21); %delay peaks
    x4=find(z22); % doppler peaks

    if sum(z21)>0,
        N1=min(x3);
    else
        N1=101;%He uses 101
    end

    if sum(z22)>0,
        N2=max(x4)+51;
    else
        N2=-101;%He uses -101
    end
    A=N1-1;B=101-N2;%He uses 101 instead of N
    if A <= B
        N12=N1;
        if N1> 50,
            alph0=1;
        else

```

```

        alph0=z21(N1);
    end

    else
        N12=N2;
        if N2 < 50,
            alph0=1;
        else
            alph0=z22(N2-51);%He uses 51
        end
    end

    N12=N12-1;
    alph0=1.0011*alph0/10;
    %End of channel estimation
else
    N12=min(delay);
    alph0=(N-min(delay))/N;
end

% Calculating error using old method
gn2=wshift('1D',gn1,N12)./alph0;
recfinal=sj.*gn2;
y=sum(real(recfinal))/(N-m);

% Comparison and BER computation for Jammer

if y>0
    dh=1;
else
    dh=-1;
end

if dh==d
    error=0;
else
    error=1;
end

errorjammer=errorjammer+error;

% Errors using LMS
mu=.05;
% First case, ERRORGN1 - Uses Jammer detection and channel
% estimation
[Agn1,Egn1] =nlms(sj,d*ones(1,N),mu,N,gn2); % Calculate LMS usi
%ng reference value = d

```



```

[A2gn1,E2gn1] =nlms(sj,-d*ones(1,N),mu,N,gn2);% Calculate LMS
%using reference value = -d

egn1=sum(abs(Egn1));
e2gn1=sum(abs(E2gn1));

if egn1<e2gn1
    erradogn1=0;
else
    erradogn1=1;
end
erradogn1s=erradogn1s+erradogn1;%

% Second, using ERRORGN - Uses channel estimation
gn2=zeros(1,101);
gn2=wshift('1D',conj(gn),N12)./alph0;

[Agn,Egn] =nlms(sj,d*ones(1,N),mu,N,gn2); % Calculate LMS using
%reference value = d
[A2gn,E2gn] =nlms(sj,-d*ones(1,N),mu,N,gn2);% Calculate LMS
%using reference value = -d

egn=sum(abs(Egn));
e2gn=sum(abs(E2gn));

if egn<e2gn
    erradogn=0;
else
    erradogn=1;
end
erradogns=erradogns+erradogn;

% Third, using gn1 no channel estimation ERRORGN1nochannel
gn2=zeros(1,101);
gn2=gn1;

[Agn1n,Egn1n] =nlms(sj,d*ones(1,N),mu,N,gn2); % Calculate LMS
%using reference value = d
[A2gn1n,E2gn1n] =nlms(sj,-d*ones(1,N),mu,N,gn2);% Calculate LMS
%using reference value = -d

egn1n=sum(abs(Egn1n));
e2gn1n=sum(abs(E2gn1n));

if egn1n<e2gn1n
    erradogn1n=0;
else

```

```

        erradogn1n=1;
    end
    erradogn1ns=erradogn1ns+erradogn1n;

    % No Jammer detection no channel estimation ERRORGNnochannel

    gn2=zeros(1,101);
    gn2=conj(gn);

    [Agnn,Egnn] =nlms(sj,d*ones(1,N),mu,N,gn2); % Calculate LMS
    %using reference value = d
    [A2gnn,E2gnn] =nlms(sj,-d*ones(1,N),mu,N,gn2);% Calculate LMS
    %using reference value = -d

    egnn=sum(abs(Egnn));
    e2gnn=sum(abs(E2gnn));

    if egnn<e2gnn
        erradognn=0;
    else
        erradognn=1;
    end
    erradognns=erradognns+erradognn;

    clear rec;
    clear REC;
    li

end
ERRORJAMMER(jsr,snr)=errorjammer;
ERRORGN1(jsr,snr)=erradogn1s;
ERRORGN(jsr,snr)=erradogns;
ERRORGN1nochannel(jsr,snr)=erradogn1ns;
ERRORGNnochannel(jsr,snr)=erradognns;
errorjammer=0;
erradogn1s=0;
erradogns=0;
erradogn1ns=0;
erradognns=0;
jsr
snr
end
end

```

BIBLIOGRAPHY

- [1] Hayes, M. H., *Statistical Signal Processing and Modeling* (New York, USA: John Wiley and Sons, Inc., 1996).
- [2] Alsheri, A. A., “Blind Estimation of Multi-path and Multi-user Spread Spectrum Channels and Jammer Excision via the Evolutionary Spectral Theory,” (unpublished Ph.D. Dissertation, School of Engineering, University of Pittsburgh, Pittsburgh, PA, 2004).
- [3] Schiller, M., *Mobile Communications* (Great Britain: Addison-Wesley, 2003).
- [4] Fazel, K. and Kaiser, S., *Multi-carrier and Spread Spectrum Systems* (1st edition; West Sussex, England: John Wiley & Sons Ltd, 2003).
- [5] S. R. Lach, M. G. Amin and Lindsey, A. R., “Broadband nonstationary interference excision for spread spectrum communications using time-frequency synthesis,” *ICASSP Proceedings*, Vol. 6 (May, 1998), pp. 3257–3260.
- [6] Chang, R. W., “Synthesis of Band Limited Orthogonal Signals for Multichannel Data Transmission,” *Bell System Tech. J.*, , No. 45 (Dec, 1996), pp. 1775–1796.
- [7] Weinstein, S. B. and Ebert, P. M., “Data Transmission by Frequency-Division Multiplexing using the Discrete Fourier Transform,” *IEEE Transactions on Communications*, Vol. 19, No. 5 (Oct, 1971), pp. 628–634.
- [8] Peled, A. and Ruiz, A., “Frequency Domain Data Transmission using Reduced Computational Complexity Algorithms,” *Proc. IEEE Int. Conf. Acoust. Speech, Signal Processing*, (April, 1980), pp. 964–967.
- [9] C. R. Nassar, Z. Wu D. Wiegandt S. A. Zekavat, B. Natarajan and Shattil, S., *Multi-Carrier Technologies for wireless Communication* (Norwell, Massachussets: Kluwer Academic Publishers, 2002).
- [10] Hara, S. and Prasad, R., “Overview of Multicarrier CDMA,” *IEEE Communications Magazine*, (Dec, 1997), pp. 126–133.
- [11] D. T. Magill, F. D. Natali and Edwards, G. P., “Spread-Spectrum Technology for Commercial Applications,” *Proceedings of the IEEE*, Vol. 82, No. 4 (April, 1994), pp. 572–584.

- [12] Kaleh, G. K., "Frequency diversity spread spectrum communications system to counter band limited Gaussian interference," *IEEE Transactions on Communications*, (July, 1996), pp. 886–893.
- [13] Tan, J. and Stuber, G., "Anti-Jamming Performance of Multi-Carrier Spread Spectrum with Constant Envelope," *IEEE Int. Conf. on Comm.*, (May, 2003), pp. 743–747.
- [14] Shankar, P. M., *Introduction to Wireless Systems* (Philadelphia, PA: John Wiley & Sons Ltd, 2002).
- [15] Pahlavan, K. and Krishnamurthy, P., *Principles of Wireless Networks* (Upper Saddle River, NJ: Prentice Hall, 2002).
- [16] M. K. Simon, R. A. Scholtz B. K. Levitt, J. K. Omura, *Spread Spectrum Communications Handbook* (United States: McGraw-Hill, Inc, 1994).
- [17] Lopatka, J., "An influence of intentional jamming signals on DSP based demodulators," *IEEE Proceedings ,Military Communications Conference, 1998. MILCOM 98*, (Oct, 1998), pp. 655–658.
- [18] T. Ristaniemi, K. Raju and Karhunen, J., "Jammer mitigation in DS-CDMA array system using independent component analysis," *IEEE International Conference on Communications*, (April, 2002), pp. 232–236.
- [19] Simon, M. K., "The performance of M-ary FH-DSPK in the presence of Partial-Band multitone jammer," *IEEE Transactions on Communications*, (May, 1982), pp. 953–958.
- [20] Ravi, K. V. and Ormondroyd, R. F., "Effect of CW and pulse jamming on direct-sequence spread-spectrum code acquisition using a sequential detector," *IEEE Proceedings, Military Communications Conference, 1992. MILCOM 92*, (Oct, 1992), pp. 638–643.
- [21] S. Senay, A. Akan and Chaparro, L.F., "Time-Frequency Channel Modeling an Estimation of Multi-Carrier Spread Spectrum Communication Systems," *ICASSP Proceedings*, (Sept, 2005), pp. 745–748.
- [22] R. Suleesathira, L. F. Chaparro and Akan, A., "Discrete Evolutionary Transform for time-frequency analysis," *J. of Franklin Institute*, (Jul, 2000), pp. 347–364.
- [23] Chaparro, L. F. and Alsheri, A. A., "Channel modeling for spread spectrum via evolutionary transform," *IEEE Int. Conf. on Acoust., Speech, and Sig. Proc., ICASSP'04*, (May, 2004), pp. 609–612.
- [24] Cohen, L., *Time-Frequency Analysis* (Upper Saddle River, New Jersey: Prentice Hall PTR, 1995).
- [25] Miller, S. L. and Rainbolt, B. J., "MMSE Detection of Multicarrier CDMA," *IEEE journal on selected areas in communications*, , No. 11 (Nov, 2000), pp. 2356–2362.

- [26] Barbosa, A. N. and Miller, S. L., “Adaptive Detection of DS/CDMA Signals in Fading Channels,” *IEEE Transactions on Communications*, (Jan, 1998), pp. 115–124.